UNIVERSIDADE FEDERAL DE VIÇOSA

NAYARA MATIKO REIS MIYASHITA

INTERAÇÃO LISOZIMA *VERSUS* CURCUMINA: TERMODINÂMICA E CINÉTICA DE FORMAÇÃO DE COMPLEXO, FOTO E TERMODEGRADAÇÃO

VIÇOSA - MINAS GERAIS
2020

NAYARA MATIKO REIS MIYASHITA

INTERAÇÃO LISOZIMA *VERSUS* CURCUMINA: TERMODINÂMICA E CINÉTICA DE FORMAÇÃO DE COMPLEXO, FOTO E TERMODEGRADAÇÃO

Dissertação apresentada à Universidade Federal de Viçosa, como parte das exigências do Programa de Pós-Graduação em Ciência e Tecnologia de Alimentos, para obtenção do título de *Magister Scientiae*.

Orientadora: Ana Clarissa dos Santos Pires

VIÇOSA - MINAS GERAIS
2020

Ficha catalográfica elaborada pela Biblioteca Central da Universidade Federal de Viçosa - Campus Viçosa

T

M685i 2020

Miyashita, Nayara Matiko Reis, 1990-
Interação lisozima versus curcumina : termodinâmica e cinética de formação de complexo, foto e termodegradação / Nayara Matiko Reis Miyashita. - Viçosa, MG, 2020.
69 f. : il. (algumas color.) ; 29 cm.

Inclui anexo.
Orientador: Ana Clarissa dos Santos Pires.
Dissertação (mestrado) - Universidade Federal de Viçosa.
Inclui bibliografia.

1. Curcumina. 2. Lisozima. 3. Interações. 4. Espectroscopia. I. Universidade Federal de Viçosa. Departamento de Tecnologia de Alimentos. Programa de Pós-Graduação em Ciência e Tecnologia de Alimentos. II. Título.

CDD 2. ed. 664.07

NAYARA MATIKO REIS MIYASHITA

INTERAÇÃO LISOZIMA *VERSUS* CURCUMINA: TERMODINÂMICA E CINÉTICA DE FORMAÇÃO DE COMPLEXO, FOTO E TERMODEGRADAÇÃO

Dissertação apresentada à Universidade Federal de Viçosa, como parte das exigências do Programa de Pós-Graduação em Ciência e Tecnologia de Alimentos, para obtenção do título de *Magister Scientiae*.

APROVADA: 20 de fevereiro de 2020.

Assentimento:

Nayara Miyashita

Nayara Matiko Reis Miyashita

Autora

Ana Clarissa dos Santos Pires

Orientadora

AGRADECIMENTOS

A Deus, por todas as bençãos recebidas diariamente, em forma de coragem, força e sabedoria pra alcançar mais esta vitória.

Aos meus pais e irmã, Edison, Ana Maria e Ana Flávia, pelo apoio e amor incondicionais.

Ao meu marido, Daniel, pelo amor sem medidas e incentivo constante.

A todos os meus professores da jornada e em especial à professora e literal orientadora, Ana Clarissa, pelos ensinamentos, apoio, disponibilidade, compreensão, confiança e amizade.

Ao professor Luis Henrique, pela coorientação, boa vontade e conhecimentos compartilhados, e também à equipe QUIVECOM pela colaboração.

À Jaqueline, por aceitar contribuir com esta banca.

Aos amigos do THERMA, as amigas da república Spartilho, aos amigos da vida e familiares, pela parceria, suporte e incentivo.

Ao Conselho Nacional de Desenvolvimento Científico e Tecnológico (CNPq) pela concessão da bolsa de estudo, à Fundação de Amparo à Pesquisa de Minas Gerais (FAPEMIG) e à Coordenação de Aperfeiçoamento de Pessoal de Nível Superior (CAPES) pelo apoio financeiro ao projeto.

À Universidade Federal de Viçosa e ao Departamento de Tecnologia de Alimentos pela oportunidade de realização do mestrado.

Meu muito obrigada a todos que contribuíram direta ou indiretamente para a conclusão deste trabalho!

RESUMO

MIYASHITA, Nayara Matiko Reis, M.Sc., Universidade Federal de Viçosa, fevereiro de 2020. **Interação lisozima *versus* curcumina: termodinâmica e cinética de formação de complexo, foto e termodegradação**. Orientadora: Ana Clarissa dos Santos Pires.

A aplicação da curcumina em sistemas aquosos é limitada, devido à sua sensibilidade à luz e à variações de temperatura, o que leva a perda de suas propriedades bioativas. Com o intuito de contornar estas limitações, a foto e termoproteção da curcumina pela lisozima foram estudadas em pH 7,4, utilizando espectroscopia de absorção molecular (UV-vis). A formação do complexo lisozima-curcumina, de estequiometria 1:1, foi confirmada por meio de análises termodinâmicas utilizando ressonância plasmônica de superfície, onde foram obtidas constantes de interação (K_b) da ordem de 10^3 $L.mol^{-1}$. Os valores de $\Delta G°$ foram todos negativos e variaram pouco com o aumento da temperatura, indicando que o equilíbrio químico favorece a formação do complexo lisozima-curcumina ($\Delta G°_{298.15\ K} = -20{,}50\ kJ\ mol^{-1}$) e a ocorrência de compensação entálpico-entrópica na formação do complexo. As alterações conformacionais da lisozima contribuíram significativamente para a formação do complexo entre estas moléculas. Os complexos termodinamicamente estáveis formaram-se via a criação de um complexo ativado. A associação das moléculas livres e a dissociação do complexo termodinamicamente estável para a formação do complexo ativado ocorreu em múltiplos-passos, com a energia de ativação dependente da temperatura. Este estudo mostrou que a formação de complexos entre lisozima e curcumina aumentou a estabilidade desta a luz e a variação de temperatura. Além disso, mostrou que a cinética e a termodinâmica de formação de complexos lisozima-curcumina é modelada pela temperatura, fornecendo parâmetros para a sua aplicação em diferentes matrizes.

Palavras-chave: Curcumina. Lisozima. Fotodegradação da curcumina. Termodegradação da curcumina. Interação termodinâmica. Constante cinética.

ABSTRACT

MIYASHITA, Nayara Matiko Reis, M.Sc., Universidade Federal de Viçosa, February, 2020. **The interaction between lysozyme and curcumin: thermodynamics and kinetics of complex formation, photo and termal degradation**. Adviser: Ana Clarissa dos Santos Pires.

The application of curcumin in aqueous systems is limited due to its high sensitivity to light and temperature flutuaction, which leads to the loss of its bioactive properties. In order to overcome these limitations, the curcumin photo and thermal protections by lysozyme were investigated at pH 7.4, using ultraviolet-visible spectrophotometry (UV-vis). The lysozyme-curcumin complex formation was confirmed by a thermodynamic analysis using surface plasmon resonance, that provided binding constants (K_b) on the order of 10^3 L mol^{-1}, with 1:1 stoichiometry. The $\Delta G°$ values were all negative and remained almost unchanged as the temperature increased, therefore, the stable complex predominated over free molecules ($\Delta G°_{298.15K} = -20.50$ kJ mol^{-1}) and the enthalpy-entropy compensation phenomenon occurred in this process. The lysozyme conformational changes were the main responsible to the lysozyme-curcumin complex formation. The association of free molecules and the dissociation of the stable complex to form an intermediate complex occurred in multi-steps, being the activation energy dependent of temperature. This study shows that the formation of a complex between curcumin and lysozyme can protect curcumin from thermal and photodegradation, providing thermodynamic and kinetic data for the better application of this complex in the food, cosmetic and pharmaceutical industry.

Keywords: Curcumin. Lysozyme interaction. Curcumin photodegradation. Curcumin thermal-degradation. Thermodynamic binding. Kinetic constants.

SUMÁRIO

1. INTRODUÇÃO

O acesso à informação tornou-se mais simples com o acelerado avanço tecnológico, acompanhado da maior acessibilidade a computadores, celulares e da popularização da internet. Entre as informações disseminadas estão as relacionadas à saúde, bem-estar e qualidade de vida. O consumidor melhor informado tende a valorizar características que vão além do preço, como sabor e qualidade nutricional dos alimentos. Para atender a esta demanda, as indústrias de alimentos tendem a otimizar as formulações dos seus produtos, incluindo ingredientes com propriedades funcionais, optando por corantes naturais e substituindo aditivos por moléculas naturais que desempenham as mesmas funções destes.

O açafrão (*Curcuma longa)*, muito utilizado na Ásia como tempero e corante, ganhou um grande destaque no cenário científico mundial em virtude de suas propriedades funcionais, como anti-inflamatória, antioxidante e antimicrobiana. A curcumina é o principal composto bioativo deste, tornando-se alvo de pesquisas não só do ramo alimentício como também farmacêutico. Porém, este composto bioativo é instável à exposição à luz, a algumas faixas de pH e temperatura (CASTILLO et al., 2015; JAGANNATHAN; ABRAHAM; PODDAR, 2012; SCHNEIDER et al., 2015). Portanto, torna-se necessário o estudo de alternativas para proteger a curcumina, mantendo suas propriedades bioativas.

A formação de complexos entre proteínas e a curcumina é uma maneira alternativa de viabilização da aplicação deste composto bioativo em formulações alimentícias, cosméticos e medicamentos. A lisozima (LYS) é uma pequena proteína globular, formada por 129 resíduos de aminoácidos, de massa molar igual 14,7 kDa, e entre as suas propriedades biológicas destaca-se a antimicrobiana (WU et al., 2019). Além disto, esta proteína é abundantemente encontrada na clara de ovos de aves e possui um custo relativamente baixo, comparado ao de outras proteínas, tornando-se assim uma potencial alternativa para interação com a curcumina (WILKEN; NIKOLOV, 2011).

Alguns estudos determinaram os parâmetros termodinâmicos de formação de complexo entre curcumina e lisozima por meio da técnica de espectroscopia de fluorescência, confirmando a formação de complexo entre estas moléculas (BORANA et al., 2014; KAMSHAD et al., 2019; LI et al., 2015; WANG; LIU; LEE, 2009). Porém,

estudos cinéticos da formação do complexo lisozima-curcumina ainda não foram realizados, nem estudos sobre a foto e termoproteção da curcumina pela lisozima.

O estudo das propriedades termodinâmicas e cinéticas dos complexos formados pela interação lisozima-curcumina, aliado ao estudo do efeito da lisozima na estabilidade à luz e ao calor da curcumina, permite o conhecimento da energética e da dinâmica molecular que governam a formação do complexo, bem como a taxa de associação de dissociação destes complexos, fornecendo informações sobre as melhores condições de aplicação destes complexos.

2. OBJETIVOS

2.1. Objetivo geral

Estudar a foto e termodegradação da curcumina na presença e ausência de lisozima, bem como a termodinâmica e cinética de formação de complexo entre a lisozima e a curcumina, em pH 7,4, em diferentes temperaturas.

2.2. Objetivos específicos

- Determinar a constante de interação (K_b), a estequiometria do complexo formado (n), a variação da energia livre de Gibbs padrão ($\Delta G°$), a variação da entalpia padrão ($\Delta H°$) e a variação da entropia padrão ($\Delta S°$) e a variação da capacidade calorífica padrão ($\Delta C_p°$) de formação do complexo lisozima–curcumina, em diferentes temperaturas, por meio da técnica de ressonância plasmônica de superfície.
- Determinar a constante de associação - K_a e a constante de dissociação - K_d dos complexos lisozima-curcumina.
- Calcular os parâmetros energéticos cinéticos de formação do complexo ativado lisozima-curcumina constituído a partir da associação das moléculas livres e a partir da dissociação do complexo termodinamicamente estável: energia de ativação (E_{act}), variação da entalpia de ativação ($\Delta H^‡$), variação da entropia de ativação ($\Delta S^‡$) e variação da energia livre de Gibbs de ativação ($\Delta G^‡$).
- Obter as constantes cinéticas de fotodegradação (K_{FD}) e termodegradação (K_{TD}) da curcumina na presença e ausência de lisozima, além do tempo de meia vida ($t_{1/2}$) da curcumina nestas mesmas condições, por meio da técnica de espectroscopia de absorção molecular (UV-vis).

3. REFERENCIAL TEÓRICO

3.1. Lisozima

A lisozima, também conhecida como muramidase, é uma proteína globular que possui propriedades antiviral, antihistamínica e antimicrobiana (NATTRESS; YOST; BAKER, 2001; PARROT; NICOT, 1963a; TAKAHASHI et al., 2018).

A característica comum das lisozimas é sua habilidade de hidrolisar a ligação glicosídica β (1-4), entre o ácido murâmico e a N-acetilglicosamina do polissacarídeo encontrado na parede celular das bactérias. Lisozimas pertencentes ao reino animal, podem ser divididas em três famílias dominantes, baseadas em suas diferentes características (sequência de aminoácidos, bioquímicas e propriedades enzimáticas): convencional ou de galinha (tipo C), de ganso (tipo G) e de invertebrados (tipo I). As lisozimas do tipo C, como a lisozima humana, são produzidas pela maioria dos vertebrados, incluindo mamíferos, aves, peixeis, reptéis e anfíbios (CALLEWAERT; MICHIELS, 2010). Tanto a lisozima humana (hLYS) quanto a lisozima de clara de ovo (LYS) são do tipo C e existe cerca de 59% de identidade entre hLYS e a LYS (CAO et al., 2015).

A lisozima (E.C.3.2.1.17), do tipo C, representa 3,9 % das proteínas presentes na clara de ovo, possui estrutura primária formada por 129 resíduos de aminoácidos, sendo a lisina a molécula N-terminal e a leucina a molécula C terminal (Figura 1). Possui caráter básico, ponto isoelétrico (PI) igual a 10,7 e sua massa molar é de 14,3 kDa, sendo estabilizada por quatro ligações dissulfeto entre os oito resíduos de cisteína (Cys) da sua cadeia polipeptídica (^{6}Cys–^{127}Cys, ^{30}Cys–^{115}Cys, ^{64}Cys–^{80}Cys e ^{76}Cys–^{94}Cys). Ainda é formada por seis resíduos de triptofano (Try), três de tirosina (Tyr) e três de fenilalanina (Phe), sendo os resíduos Try-62 e Try-108 considerados os principais fluoróforos na lisozima (IMOTO et al., 1971; WU et al., 2019). Esta molécula é um elipsoide de 4,5 x 3,0 x 3,0 nm, e seu interior é altamente hidrofóbico (LESNIEROWSKI; STANGIERSKI, 2018a).

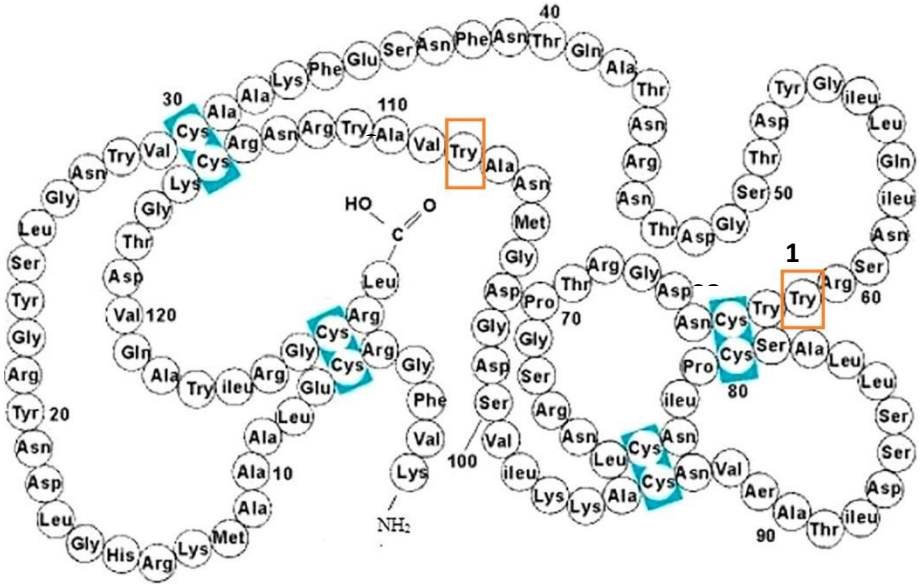

Figura 1- Estrutura da Lisozima Fonte: Wu et al., 2019.

Esta proteína possui alto valor agregado devido às propriedades supracitadas, e vem sendo utilizada em diversas aplicações industriais, como em soluções oftalmológicas, remédios para úlceras e infecções, agente para extração de produtos intracelulares bacterianos, na preservação de alimentos, produção de queijos, fórmulas infantis e na clarificação de bebidas e vinhos (GHOSH; CUI, 2000; LESNIEROWSKI; STANGIERSKI, 2018a). Outro campo de aplicação da lisozima é como proteína carreadora de diferentes moléculas, pois é capaz de interagir com pequenas drogas farmacêuticas, sendo importante o estudo de transporte e do processo metabólico da droga (DAS et al., 2017), bem como trabalhos relacionados à compreensão dos parâmetros relacionados à termodinâmica e cinética de interação proteína-ligante.

Pesquisas na área farmacêutica utilizaram a lisozima com o propósito de avaliar a eficácia da curcumina como molécula inibidora da formação de amilóides em humanos. WANG, LIU, e LEE (2009) estudaram a termodinâmica de formação de complexo entre lisozima e curcumina, por meio de espectroscopia de fluorescência, em pH 2, onde os valores da variação da energia livre de Gibbs ΔG determinada a constante de ligação (K_b) nas temperaturas de 10 a 55 ºC, obtendo valores da ordem de 10^4 M^{-1} até 45ºC e da ordem de 10^3 M^{-1} a 55 ºC, sendo o processo entalpicamente dirigido (ΔH= −78390,7 J/mol e ΔS= −169,17J/mol) e as principais forças de interação seriam Van der Walls e ligação de hidrogênio. A formação de fibrilas amiloides foi inibida pela curcumina, proporcionalmente a dose deste polifenol adicionada, sendo

que uma redução expressiva (>80%) na quantidade de fibrilas amiloides foi observada para concentrações de curcumina maiores que 50 µM.

BORANA et al. (2014) também estudaram a inibição da formação de fibrilas amiloides pela curcumina, bem como a interação de curcumina com lisozima utilizando a técnica de espectroscopia de fluorescência, em pH 7,4, a 25 ºC. A adição da curcumina à proteína ocasionou extinção de fluorescência pelo mecanismo de supressão estático, devido a formação de complexos entre a proteína e a curcumina, com K_b da ordem de $10^4\ M^{-1}$ e estequiometria igual 1. Além disso, por meio da análise de fluorescência ThT, uma diminuição na amplitude (parâmetro cinético de formação de fibrilas amiloides), sugeriu que a adição de curcumina diminuiu a quantidade de agregados amiloides formados.

MOHAMMADI et al. (2016) estudaram a capacidade da lisozima como carreadora de curcumina por meio de medidas de supressão de fluorescência, dicroísmo circular e docking molecular, em pH 6,4, nas temperaturas de 20, 25 e 30 ºC. A adição da solução de curcumina promoveu a extinção da fluorescência da lisozima, sendo o mecanismo de supressão estático. O K_b foi da ordem de $10^4\ M^{-1}$ e a estequiometria de formação do complexo igual a 1, sendo o processo entalpicamente dirigido (ΔH= -59,00 $kJ.mol^{-1}$ e ΔS= - 117,83 $kJ.mol^{-1}$).

KAMSHAD et al. (2019) estudaram as interações entre lisozima e curcumina, e entre lisozima, curcumina e nanopartículas de prata de diferentes tamanhos, com o auxílio das técnicas de UV-Vis, espectroscopia de fluorescência, espectroscopia de fluorescência sincronizada, dicroísmo circular, RLS (Resonance Light Scattering - Espalhamento de Luz Ressonante) e potencial zeta, a 25ºC, em pH 7,4. Os resultados das análises de fluorescência apresentaram um red-shift, o que indicada que um ou mais triptofanos da proteína foram expostos a um ambiente mais hidrofílico devido a interação da lisozima com a curcumina ou deste sistema binário com as nanopartículas de prata, sugerindo formação de complexo em ambos os sistemas. Foram determinados os valores de Kq ($> 2x10^{10}\ M^{-1}s^{-1}$) e $n \cong 1$ para ambos os sistemas, demonstrando que com ou sem a presença de nanopartículas de prata, havia apenas um sítio de ligação disponível para a curcumina na lisozima.

3.2. Curcumina

A *Curcuma longa*, conhecida como açafrão-da-índia, é utilizada como tempero, corante e erva medicinal na Ásia, devido às suas propriedades antioxidante, anti-

inflamatória, antimutagênica, antimicrobiana, antiviral e anticâncer. Dentre seus componentes, a curcumina se destaca como seu principal composto, pertencente ao grupo dos curcuminóides (GHAYOUR et al., 2019; MATHEW; HSU, 2018; PU et al., 2019). Este grupo corresponde a 5% dos componentes totais da *Curcuma longa,* sendo a curcumina o mais abundante composto do grupo dos curcuminóides (60-70%), seguida da demetoxicurcumina (20-27%), bisdemetoxicurcumina (10-15%) e ciclocurcumina (1-2%) (PULIDO-MORAN; MORENO-FERNANDEZ; RAMIREZ-TORTOSA, CESAR RAMIREZ-TORTOSA, 2016; SANPHUI; BOLLA, 2018).

A curcumina (1,7-bis (4-hidroxi-3-metoxifenil) -1,6-heptadieno-3,5-diona), também chamada diferulometano (Figura 2) é praticamente insolúvel em água a pH neutro e pouco ácido, e solúvel em solventes orgânicos polares e apolares, sendo mais solúvel em solventes a pH alcalino e extremamente ácido.

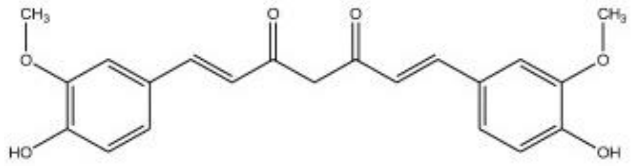

Figura 2- Estrutura química da curcumina. Fonte: MOHAMMADI e MOEENI, 2015.

Em solução, há um equilíbrio entre dois tautômeros da curcumina, chamado de equilíbrio ceto-enólico, que ocorre devido à sua porção β-dicetona. A forma com que a curcumina se encontrará depende das características do solvente, temperatura, polaridade e se há substituições na curcumina. Entretanto, geralmente a temperatura ambiente, a forma enólica é predominante (PATRA; BARAKAT, 2011; SANPHUI; BOLLA, 2018).

Este polifenol se apresenta sob a forma de um composto cristalino amarelo/alaranjado, utilizado como corante na indústria de alimentos, sendo aplicado em uma ampla variedade de produtos como margarinas, macarrões, mostardas, sorvetes, queijos e salgadinhos tipo “chips”. É seguro até mesmo em altas doses (8–12 g/dia), porém sua eficácia clínica é limitada por sua baixa solubilidade em água (7,9 mg/L) e biodisponibilidade (meia vida curta, de apenas 30-45 minutos) (SANPHUI; BOLLA, 2018).

Aliada a baixa biodisponibilidade e solubilidade em meio aquoso, a curcumina ainda apresenta alta sensibilidade à oxidação, e instabilidade durante o

armazenamento, sendo estes grandes desafios para o desenvolvimento de formulações alimentícias funcionais (PU et al., 2019). Com o objetivo de contornar estes obstáculos, muitos veículos carreadores para a curcumina foram propostos, como proteínas, lipossomos e carboidratos (NAKSURIYA et al., 2014).

Sistemas que utilizam proteínas como carreadoras de curcumina vêm sendo extensamente estudados. Foram realizados estudos da interação entre curcumina e hemoglobina (HEGDE; SANDHYA; SEETHARAMAPPA, 2013), soro albumina bovina (BSA) (HUDSON et al., 2018), ovoalbumina (LIU et al., 2017b), caseínas (GHAYOUR et al., 2019), α-lactoalbumina (MOHAMMADI; MOEENI, 2015) e lisozima (LI et al., 2015).

LI et al. (2015) estudaram a influência dos coacervatos de lisozima e carboximetilcelulose na interação e estabilidade da curcumina encapsulada nestes, bem como sua implicação na propriedade antioxidante da curcumina, por meio das técnicas de UV-Vis, fluorescência, fluorescência síncrona e dicroísmo circular. Os resultados indicam a formação de coacervatos de lisozima com carboximetilcelulose por meio de interações eletrostáticas, o que levou a um desdobramento da lisozima no coacervato, fornecendo à curcumina um ambiente mais hidrofóbico do que o da interação com lisozima livre. Ocorreu supressão de fluorescência da lisozima com adição de curcumina, sendo $K_b = 9{,}8x10^3\ M^{-1}$. Além disso, ocorreram alterações na estrutura secundária da lisozima, especialmente na estrutura α-hélice. Em relação à atividade antioxidante dos compostos formados, tanto os coacervatos de lisozima, carboximetilcelulose e curcumina quanto os complexos de lisozima e curcumina aumentam a atividade antioxidante da curcumina em pH 6,0, antes e depois do tratamento térmico.

3.3. Técnicas experimentais para estudos termodinâmicos e cinéticos

3.3.1 Avaliação da degradação cinética da curcumina por exposição à luz e ao calor

A exposição da curcumina a luz leva a produtos de degradação que podem afetar a saúde dos consumidores e alterar as propriedades sensoriais dos alimentos (NADI et al., 2015; SCHNEIDER et al., 2015). Para contornar estas limitações, vêm sendo desenvolvidas alternativas para proteção de compostos bioativos, pela formação de complexos entre estes compostos e diversos carreadores, como

proteínas, carboidratos e lipossomos (CASTILLO et al., 2015; HUDSON et al., 2018; PU et al., 2019).

SILVA et al. (2018) estudaram a fotodegradação do β-caroteno e obtiveram que o tempo de meia vida deste composto aumentou mais de 3 vezes quando este estava complexado com a BSA e mais de 4 vezes quando complexado com micelas de β-caseína, concluindo que estas proteínas podem proteger o β-caroteno da fotodegradação. HUDSON et al. (2018) observaram que o tempo de meia vida da curcumina aumentou 3 vezes após interação com a BSA (25μM), sugerindo que quando a curcumina interage com regiões hidrofóbicas da BSA, esta pode proteger este composto dos efeitos de degradação causados pela luz. HUDSON et al. (2019) estudaram a termodegradação da curcumina, e concluíram que o tempo de meia vida desta molécula, quando complexada com a caseína micelar, aumentou 2,5 vezes nas temperaturas de 30 e 40 ºC e 1,45 vezes nas temperaturas de 50 e 60ºC,quando comparado ao tempo de meia vida da curcumina pura em solução. Assim, a termodegradação da curcumina foi reduzida após a interação com a caseína micelar. Os estudos anteriormente citados reforçam que a investigação da termo e fotodegradação da curcumina são fatores importantes na aplicação industrial dos complexos formados entre curcumina e proteína.

Análises cinéticas são técnicas úteis para o estudo da estabilidade térmica e fotoquímica dos compostos bioativos, as quais tem uma aplicação prática na predição de taxas de processos, termo estabilidade, foto estabilidade e tempo de meia vida (CASTILLO et al., 2015; CHEN et al., 2014). A espectroscopia de absorção no UV-VIS é uma técnica de baixo custo operacional, fácil utilização e que produz resultados de interpretação geralmente bastante simples. Em um experimento de avaliação da degradação cinética da curcumina, são realizadas medidas da absorbância de soluções de curcumina, na ausência e presença de diferentes concentrações de proteínas, ao longo do tempo de exposição à luz (fotodegradação) e ao calor (termodegradação). A partir dos dados obtidos são determinados parâmetros importantes para estimar a estabilidade da curcumina devido à exposição à luz e ao calor. Utilizando a equação 1 determina-se K_X , a constante de fotodegradação (K_{FD}) ou de termodegradação (K_{TD}) , por meio da construção de um gráfico de $-\ln\frac{A}{A_0}$ em

função do tempo de exposição à luz. O tempo de meia vida ($t_{1/2}$) da curcumina é então determinado pela Equação 2 (HUDSON et al., 2018).

$$-\ln\frac{A}{A_0} = K_X t \quad (1)$$

$$t_{1/2} = \frac{ln2}{K_{FD}} \quad (2)$$

Onde A e A_0 são as absorbâncias no tempo final e inicial, respectivamente. E t é o tempo de exposição à luz.

3.3.2. Estudo termodinâmico e cinético de formação de complexo por meio da técnica de ressonância plasmônica de superfície (SPR)

A SPR é uma ferramenta importante no estudo de interações intermoleculares entre proteínas e moléculas bioativas, em virtude da associação e dissociação molecular serem monitoradas em tempo real, possibilitando a determinação de parâmetros cinéticos e termodinâmicos de interação (LIU et al., 2017a). Nesta técnica, a presença de marcadores nas moléculas que interagem é dispensável, ao contrário da técnica de espectroscopia de fluorescência, onde é necessário que ao menos uma das moléculas possua fluoróforos em sua estrutura.

Esta técnica ótica é baseada em alterações nos valores do índice de refração na vizinhança das camadas de metal de um chip sensor, em resposta às interações intermoleculares (NGUYEN et al., 2015). Em um experimento de interação entre uma proteína e uma molécula bioativa por meio desta técnica, a proteína é imobilizada em um chip sensor composto por uma camada de ouro, enquanto a molécula bioativa se encontra em solução. Um fluxo de soluções com concentrações diferentes da molécula bioativa entra em contato com a proteína no chip sensor, permitindo que a interação ocorra (DAY et al., 2013), e consequentemente ocorre também a variação no valor do índice de refração na superfície do chip sensor.

Um sinal de resposta ressonante (RU), gerado em função do tempo, é utilizado para expressar a mudança no índice de refração, após cada injeção da solução de

moléculas bioativas sobre o chip sensor, originando um sensograma (Figura 3) (NGUYEN et al., 2015).

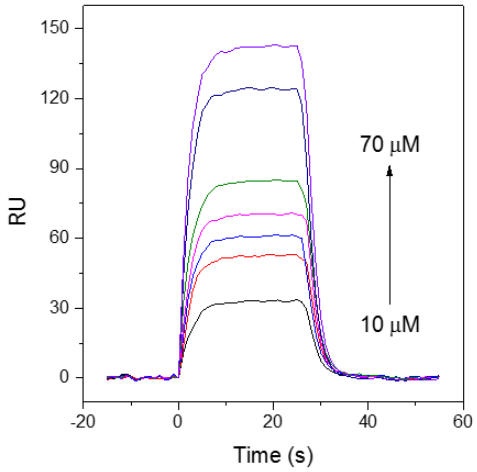

Figura 3- Sensogramas (RU x Tempo) da interação lisozima-curcumina, onde cada curva representa uma concentração do ligante.

Cada curva típica de um sensograma de interação monovalente entre uma proteína e um ligante pode ser dividida em duas regiões, como ilustrado na Figura 3. Na região 1, RU cresce durante a fase de associação (desde o tempo de injeção, t_0), devido à associação e dissociação simultânea entre ligante e a proteína imobilizada, com as interações intermoleculares ocorrendo em taxas mais elevadas, atingindo um valor experimental máximo no tempo de ressonância (t_m). Após este tempo, os valores de RU decrescem com o aumento do tempo devido à dissociação do complexo proteína-ligante, causada pelo fluxo do tampão sobre a proteína imobilizada (região 2) (DE PAULA et al., 2017).

A interação entre uma proteína (P) e um ligante (L) pode ser considerada uma reação de interação monovalente, (P + L ↔ P-L), com constante de associação (K_a) e dissociação (K_d). A fim de calcular a constante observada (K_{obs}) e K_d, os sensogramas obtidos podem ser ajustados às equações (3) e (4) (DE PAULA et al., 2017).

$$RU\ (t) = RU_{máx}[1 - e^{-K_{obs}(t)}] \quad (3)$$

$$RU\ (t) = RU\ (t_m)\ e^{-K_d(t-t_m)} \quad (4)$$

Em baixas concentrações do ligante, o valor de K_{obs} Equação (5) é linearmente dependente da concentração do ligante, [ligante], permitindo o cálculo de K_a pela inclinação da curva do gráfico de K_{obs} versus [ligante].

$$K_{obs} = K_a\,[\text{ligante}] + K_d \tag{5}$$

Realizando-se este experimento a diferentes temperaturas, é possível a construção do gráfico de Arrhenius, plotando-se ln K_a ou ln K_d versus 1/T. Por meio deste gráfico é determinada a energia de ativação (E_a) formada a partir da associação das moléculas livres ($E_{a(a)}$) ou da dissociação do complexo termodinamicamente estável ($E_{a(d)}$), para o processo de formação de complexo ativado, por meio da Equação (6).

$$E_{a(y)}(T) = -R\left(\frac{d\ln K(y)}{dT}\right) \tag{6}$$

Onde o ‘’y’’ subescrito poderá significar a fase de associação ou de dissociação, sendo substituído por ‘’a’’ ou ‘’d’’, respectivamente. $E_{a(y)}$ (T) é a energia de ativação (kJ/mol), R é a constante universal dos gases (8,3145 J/mol.K) e K_y é a constante de associação (K_a) ($M^{-1}.s^{-1}$) ou dissociação (K_d) (s^{-1}).

A partir da determinação do valor da $E_{a(y)}$, são determinados os valores da variação da energia livre de Gibbs de ativação, $\Delta G_y^{\ddagger}(T)$, a variação da entalpia de ativação $\Delta H_y^{\ddagger}(T)$ e a variação da entropia de ativação $\Delta S_y^{\ddagger}(T)$ para formação de complexo ativado a partir da associação de moléculas livres (y=a) ou da dissociação do complexo (y=d), por meio das Equações (7), (8) e (9), respectivamente.

$$\Delta G_y^{\ddagger}(T) = -RTln\,\frac{K_y h}{K_B T} \tag{7}$$

$$\Delta H_y^{\ddagger}(T) = E_{a(y)}(T) - RT \tag{8}$$

$$T\Delta S_y^{\ddagger}(T) = \Delta H_y^{\ddagger}(T) - \Delta G_y^{\ddagger}(T) \tag{9}$$

Onde h é a constante de Plank, K_B é a constante de Boltzmann, R é a constante universal dos gases e a T é a temperatura (K).

Os parâmetros termodinâmicos também podem ser determinados conhecendo-se os valores das constantes cinéticas K_a e K_d. A constante de ligação entre a proteína e o ligante (K_b) é obtida por meio da relação $K_b = K_a/K_d$.

Conhecendo o valor de K_b, é obtida a variação da energia livre de Gibbs padrão de formação de complexo, $\Delta G°$, por meio da equação 10 (NUNES et al., 2017).

$$\Delta G° = -RT\ ln\ K_b \quad (10)$$

Onde R é a constante universal dos gases (8,314 J/mol K) e T é a temperatura (K).

$\Delta G°$ possui duas componentes, uma entálpica ($\Delta H°$) e outra entrópica ($T\Delta S°$) (Equação 11). O sinal e a magnitude dessas contribuições na formação do complexo podem fornecer informações sobre as principais forças envolvidas no processo de ligação. Para a determinação do termo entálpico é utilizada a equação de Van't Hoff (Equação 12), com os dados de um experimento de fluorescência realizado em diferentes temperaturas, seguido da análise do gráfico de $ln\ K_b$ versus $1/T$. O termo entrópico é então obtido por meio da Equação 11 (CHENG, 2012; HUDSON et al., 2018).

$$\Delta G° = \Delta H° - T\Delta S° \quad (11)$$

$$\frac{\ln K_{b2}}{\ln K_{b1}} = -\frac{\Delta H°}{R}\left(\frac{1}{T_1} + \frac{1}{T_2}\right) \quad (12)$$

onde $\Delta H°$ (kJ/mol) é a variação da entalpia padrão de formação de complexo, $\Delta S°$ (kJ/mol) é a variação da entropia padrão de formação de complexo, K_b (L/mol) é a constante de ligação, T é a temperatura e R (8,314 J/mol K) é a constante universal dos gases.

4. REFERÊNCIAS BIBLIOGRÁFICAS

ALLEN, B. et al. A Ligand-induced , Change in Penicillopepsin. **The Journal of Biological Chemistry**, v. 265, n. 9, p. 5060–5065, 1990.

APARICIO-RUIZ, R.; MÍNGUEZ-MOSQUERA, M. I.; GANDUL-ROJAS, B. Thermal degradation kinetics of lutein, β-carotene and β-cryptoxanthin in virgin olive oils. **Journal of Food Composition and Analysis**, v. 24, n. 6, p. 811–820, set. 2011.

ARIYARATHNA, I. R.; KARUNARATNE, D. N. Microencapsulation stabilizes curcumin for efficient delivery in food applications. **Food Packaging and Shelf Life**, v. 10, p. 79–86, dez. 2016.

BORANA, M. S. et al. Curcumin and kaempferol prevent lysozyme fibril formation by modulating aggregation kinetic parameters. **Biochimica et Biophysica Acta - Proteins and Proteomics**, v. 1844, n. 3, p. 670–680, 2014.

BOURASSA, P. et al. Resveratrol , Genistein , and Curcumin Bind Bovine Serum Albumin †. **Journal of Physical Chemistry B**, v. 114, p. 3348–3354, 2010.

CALLEWAERT, L.; MICHIELS, C. W. Lysozymes in the animal kingdom. **Journal of Biosciences**, v. 35, n. 1, p. 127–160, 23 mar. 2010.

CAO, D. et al. Expression of Recombinant Human Lysozyme in Egg Whites of Transgenic Hens. **PLOS ONE**, v. 10, n. February 2015, p. 1–15, 2015.

CASTILLO, M. L. R. DEL et al. Stabilization of curcumin against photodegradation by encapsulation in gamma-cyclodextrin: A study based on chromatographic and spectroscopic (Raman and UV–visible) data. **Vibrational Spectroscopy**, v. 81, p. 106–111, nov. 2015.

CEGIELSKA-RADZIEJEWSKA, R.; SZABLEWSKI, T. Effect of Modified Lysozyme on the Microflora and Sensory Attributes of Ground Pork. **Journal of Food Protection**, v. 76, n. 2, p. 338–342, 2013.

CHEN, L. J.; LIN, S. Y.; HUANG, C. C. Effect of hydrophobic chain length of surfactants on enthalpy-entropy compensation of micellization. **Journal of Physical Chemistry B**, v. 102, n. 22, p. 4350–4356, 28 maio 1998.

CHEN, Z. et al. Thermal degradation kinetics study of curcumin with nonlinear methods. **Food Chemistry**, v. 155, p. 81–86, jul. 2014.

CHENG, Z. Studies on the interaction between scopoletin and two serum albumins by spectroscopic methods. **Journal of Luminescence**, v. 132, p. 2719–2729, 2012.

COELHO, Y. L. et al. Lactoferrin-phenothiazine dye interactions: Thermodynamic and kinetic approach. **International Journal of Biological Macromolecules**, v. 136, p. 559–569, 1 set. 2019.

DAS, S. et al. Binding of naringin and naringenin with hen egg white lysozyme: A spectroscopic investigation and molecular docking study. **Spectrochimica Acta - Part A: Molecular and Biomolecular Spectroscopy**, v. 192, p. 211–221, 2017.

DAY, E. S. et al. Determining the affinity and stoichiometry of interactions between unmodified proteins in solution using Biacore. **Analytical Biochemistry Journal**, v. 440, p. 96–107, 2013.

DE PAULA, H. M. C. et al. Kinetics and thermodynamics of bovine serum

albumin interactions with Congo red dye. **Colloids and Surfaces B: Biointerfaces**, v. 159, n. 2017, p. 737–742, 2017.

ERCAN, D.; DEMIRCI, A. **Recent advances for the production and recovery methods of lysozymeCritical Reviews in Biotechnology**Taylor and Francis Ltd, , 1 nov. 2016.

FATHI, F. et al. Kinetic studies of bovine serum albumin interaction with PG and TBHQ using surface plasmon resonance. **International Journal of Biological Macromolecules**, v. 91, p. 1045–1050, out. 2016.

FOX, J. M. et al. The Molecular Origin of Enthalpy/Entropy Compensation in Biomolecular Recognition. **Annual Review of Biophysics**, v. 47, n. 1, p. 223–250, 2018.

GHAYOUR, N. et al. Nanoencapsulation of quercetin and curcumin in casein-based delivery systems. **Food Hydrocolloids**, v. 87, n. March 2018, p. 394–403, 2019.

GHOSH, R.; CUI, Z. F. Purification of Lysozyme Using Ultrafiltration. **Biotechnology and Bioengineering**, v. 68, p. 191–203, 2000.

GUPTA, S. C. et al. **Regulation of survival, proliferation, invasion, angiogenesis, and metastasis of tumor cells through modulation of inflammatory pathways by nutraceuticalsCancer and Metastasis Reviews**, set. 2010.

GUPTA, S. C. et al. Multitargeting by curcumin as revealed by molecular interaction studies. **Natural Product Reports - Royal Society of Chemistry**, v. 28, p. 1937–1955, 2011.

HEGDE, A. H.; SANDHYA, B.; SEETHARAMAPPA, J. Investigations to reveal the nature of interactions of human hemoglobin with curcumin using optical techniques ☪. **International Journal of Biological Macromolecules**, v. 52, n. January 2012, p. 133–138, 2013.

HUDSON, E. A. et al. Thermodynamic and kinetic analyses of curcumin and bovine serum albumin binding. **Food Chemistry**, v. 242, n. August 2017, p. 505–512, 2018.

HUDSON, E. A. et al. Curcumin micellar-casein multisite interactions elucidated by surface plasmon resonance. **International Journal of Biological Macromolecules**, v. 133, n. July 2019, p. 860–866, 2019a.

HUDSON, E. A. et al. Energetic parameters of β-casein/quercetin activated and thermodynamically stable complex formation accessed by Surface Plasmon Resonance. **Colloids and Surfaces B: Biointerfaces**, v. 181, n. June, p. 798–805, 2019b.

IMOTO, T. et al. Fluorescence of Lysozyme : Emissions from Tryptophan Residues 62 and 108 and Energy Migration. **Proceedings of the National Academy of Sciences of the United States of America**, v. 69, n. 5, p. 1151–1155, 1971.

JAGANNATHAN, R.; ABRAHAM, P. M.; PODDAR, P. Temperature-dependent spectroscopic evidences of curcumin in aqueous medium: A mechanistic study of its solubility and stability. **Journal of Physical Chemistry B**, v. 116, n. 50, p. 14533–14540, 2012.

KAMSHAD, M. et al. Use of spectroscopic and zeta potential techniques to

study the interaction between lysozyme and curcumin in the presence of silver nanoparticles at different sizes. **Journal of Biomolecular Structure and Dynamics**, v. 37, n. 8, p. 2030–2040, 2019.

KUNWAR, A. et al. Transport of liposomal and albumin loaded curcumin to living cells: An absorption and fluorescence spectroscopic study. **Biochimica et Biophysica Acta - General Subjects**, v. 1760, n. 10, p. 1513–1520, out. 2006.

LESNIEROWSKI, G.; STANGIERSKI, J. Trends in Food Science & Technology What ' s new in chicken egg research and technology for human health promotion ? - A review. **Trends in Food Science & Technology**, v. 71, n. June 2016, p. 46–51, 2018a.

LESNIEROWSKI, G.; STANGIERSKI, J. What's new in chicken egg research and technology for human health promotion? - A review. **Trends in Food Science and Technology**, v. 71, n. October 2017, p. 46–51, 2018b.

LI, Z. et al. Curcumin encapsulated in the complex of lysozyme / carboxymethylcellulose and implications for the antioxidant activity of curcumin. **Food Research International**, v. 75, p. 98–105, 2015.

LIU, X. et al. Investigation of the interaction for three Citrus flavonoids and α -amylase by surface plasmon resonance. **Food Research International**, v. 97, p. 1–6, 2017a.

LIU, Y. et al. Improved antioxidant activity and physicochemical properties of curcumin by adding ovalbumin and its structural characterization. **Food Hydrocolloids**, v. 72, p. 304–311, 2017b.

LIU, Y. et al. Ovalbumin as a carrier to significantly enhance the aqueous solubilityand photostability of curcumin: Interaction and bindingmechanism study. **International Journal of Biological Macromolecules**, v. 116, n. May 2018, p. 893–900, 2018.

MAŁACZEWSKA, J. et al. Antiviral effects of nisin, lysozyme, lactoferrin and their mixtures against bovine viral diarrhoea virus. **BMC Veterinary Research**, v. 15, n. 1, p. 1–12, 2019.

MANDEVILLE, J. S.; FROEHLICH, E.; TAJMIR-RIAHI, H. A. Study of curcumin and genistein interactions with human serum albumin. **Journal of Pharmaceutical and Biomedical Analysis**, v. 49, n. 2, p. 468–474, 20 fev. 2009.

MATHEW, D.; HSU, W. Antiviral potential of curcumin. **Journal of Functional Foods**, v. 40, n. September 2017, p. 692–699, 2018.

MOHAMMADI, F. et al. Interaction of curcumin and diacetylcurcumin with the lipocalin member β-lactoglobulin. **Protein Journal**, v. 28, n. 3–4, p. 117–123, maio 2009.

MOHAMMADI, F. et al. Inhibition of amyloid fibrillation of hen egg-white lysozyme by the natural and synthetic curcuminoids. **RSC Advances**, v. 6, n. 28, p. 23148–23160, 2016.

MOHAMMADI, F.; MOEENI, M. Study on the interactions of trans-resveratrol and curcumin with bovine α -lactalbumin by spectroscopic analysis and molecular docking. **Materials Science and Engineering C**, v. 50, p. 358–366, 2015.

MONDAL, S.; GHOSH, S.; MOULIK, S. P. Stability of curcumin in different solvent and solution media: UV–visible and steady-state fluorescence spectral study.

Journal of Photochemistry and Photobiology B: Biology, v. 158, p. 212–218, 2016.

NADI, M. M. et al. Comparative Spectroscopic Studies on Curcumin Stabilization by Association to Bovine Serum Albumin and Casein: A Perspective on Drug-Delivery Application. **International Journal of Food Properties**, v. 18, n. 3, p. 638–659, 4 mar. 2015.

NAKSURIYA, O. et al. Curcumin nanoformulations : A review of pharmaceutical properties and preclinical studies and clinical data related to cancer treatment. **Biomaterials**, v. 35, p. 3365–3383, 2014.

NAKSURIYA, O. et al. A kinetic degradation study of curcumin in its free form and loaded in polymeric micelles. **AAPS Journal**, v. 18, n. 3, p. 777–787, 2016.

NATTRESS, F. M.; YOST, C. K.; BAKER, L. P. Evaluation of the ability of lysozyme and nisin to control meat spoilage bacteria. **International Journal of Food Microbiology**, v. 70, n. 1–2, p. 111–119, 22 out. 2001.

NEGI, P. S. et al. Antibacterial Activity of Turmeric Oil A Byproduct from Curcumin Manufacture - Journal of Agricultural and Food Chemistry (ACS Publications). **J. Agric. Food Chem**, v. 47, p. 4297−4300, 1999.

NGUYEN, H. H. et al. Surface Plasmon Resonance: A Versatile Technique for Biosensor Applications. **Sensors**, v. 15, p. 10481–10510, 2015.

NIGEN, M. et al. Temperature affects the supramolecular structures resulting from α-lactalbumin - Lysozyme interaction. **Biochemistry**, v. 46, n. 5, p. 1248–1255, 2007.

NUNES, N. M. et al. Interaction of cinnamic acid and methyl cinnamate with bovine serum albumin: A thermodynamic approach. **Food Chemistry**, v. 237, n. 2017, p. 525–531, 2017.

NUNES, N. M. et al. Surface plasmon resonance study of interaction between lactoferrin and naringin. **Food Chemistry**, v. 297, n. April, p. 125022, 2019.

PAIVA, P. H. C. et al. Influence of protein conformation and selected Hofmeister salts on bovine serum albumin/lutein complex formation. **Food Chemistry**, v. 305, p. 125463, 1 fev. 2020.

PAN, Y. et al. Effect of barrier properties of zein colloidal particles and oil-in-water emulsions on oxidative stability of encapsulated bioactive compounds. **Food Hydrocolloids**, v. 43, p. 82–90, 1 jan. 2015.

PARROT, J.-L.; NICOT, G. Antihistaminic Action of Lysozyme. **Nature**, v. 197, n. February 2, p. 496, 1963a.

PARROT, J.-L.; NICOT, G. Antihistaminic Action of Lysozyme. **Nature**, v. 197, n. February 1963, p. 496, 1963b.

PATRA, D.; BARAKAT, C. Molecular and Biomolecular Spectroscopy Synchronous fluorescence spectroscopic study of solvatochromic curcumin dye. **Spectrochimica Acta Part A**, v. 79, p. 1034–1041, 2011.

PRASAD, S.; TYAGI, A. K.; AGGARWAL, B. B. **Recent developments in delivery, bioavailability, absorption and metabolism of curcumin: The golden pigment from golden spiceCancer Research and Treatment**, 2014.

PU, C. et al. Stability enhancement efficiency of surface decoration on

curcumin-loaded liposomes : Comparison of guar gum and its cationic counterpart. **Food Hydrocolloids**, v. 87, n. April 2018, p. 29–37, 2019.

PULIDO-MORAN, M.; MORENO-FERNANDEZ, J.; RAMIREZ-TORTOSA, CESAR RAMIREZ-TORTOSA, M. Curcumin and Health. **Molecules**, v. 21, n. 3, p. 1–22, 2016.

PULLA REDDY, A. C. et al. Interaction of curcumin with human serum albumin—A spectroscopic study. **Lipids**, v. 34, n. 10, p. 1025–1029, out. 1999.

REZENDE, J. DE P. et al. Thermodynamic and kinetic study of epigallocatechin-3-gallate-bovine lactoferrin complex formation determined by surface plasmon resonance (SPR): A comparative study with fluorescence spectroscopy. **Food Hydrocolloids**, v. 95, p. 526–532, 1 out. 2019.

REZENDE, J. DE P. et al. Human serum albumin-resveratrol complex formation: Effect of the phenolic chemical structure on the kinetic and thermodynamic parameters of the interactions. **Food Chemistry**, v. 307, p. 125514, mar. 2020.

SAHU, A.; KASOJU, N.; BORA, U. Fluorescence Study of the Curcumin-Casein Micelle Complexation and Its Application as a Drug Nanocarrier to Cancer Cells. **Biomacromolecules**, v. 9, p. 2905–2912, 2008.

SANPHUI, P.; BOLLA, G. Curcumin , a Biological Wonder Molecule : A Crystal Engineering Point of View. **Crystal Growth & Design**, v. 18, p. 5690–5711, 2018.

SCHNEIDER, C. et al. Stability of curcumin in buffer solutions and characterization of its degradation products. **Journal of Pharmaceutical and Biomedical Analysis**, v. 15, n. 12, p. 7606–7614, 2015.

SILVA, C. E. L. et al. β-Carotene and Milk Protein Complexation: a Thermodynamic Approach and a Photo Stabilization Study. **Food and Bioprocess Technology**, v. 11, n. 3, p. 610–620, 2018.

SILVA, L. H. M. DA et al. PEO-[M(CN)5NO]x- (M) Fe, Mn, or Cr) Interaction as a Driving Force in the Partitioning of the Pentacyanonitrosylmetallate Anion in ATPS: Strong Effect of the Central Atom. v. 1, p. 11669–11678, 2008.

SNEHARANI, A. H. et al. Interaction of curcumin with ß-lactoglobulin;stability, spectroscopic analysis, and molecular modeling of the Complex. **Journal of Agricultural and Food Chemistry**, v. 58, n. 20, p. 11130–11139, 27 out. 2010.

TAKAHASHI, M. et al. Heat-denatured lysozyme could be a novel disinfectant for reducing hepatitis A virus and murine norovirus on berry fruit. **International Journal of Food Microbiology**, v. 266, n. July 2017, p. 104–108, 2018.

VIEIRA, E. D.; BASSO, L. G. M.; COSTA-FILHO, A. J. Biochimica et Biophysica Acta Non-linear van ' t Hoff behavior in pulmonary surfactant model membranes. **BBA - Biomembranes**, v. 1859, n. 6, p. 1133–1143, 2017.

WANG, S.; LIU, K.; LEE, W. Effect of curcumin on the amyloid fibrillogenesis of hen egg-white lysozyme. **Biophysical Chemistry**, v. 144, n. 1–2, p. 78–87, 2009.

WANG, Y.-Q.; CHEN, T.-T.; ZHANG, H.-M. Investigation of the interactions of lysozyme and trypsin with biphenol A using spectroscopic methods. **Spectrochimica Acta Part A: Molecular and Biomolecular Spectroscopy**, v. 75, n. 3, p. 1130–1137, mar. 2010.

WILKEN, L. R.; NIKOLOV, Z. L. Process evaluations and economic analyses of recombinant human lysozyme and hen egg-white lysozyme purifications.

Biotechnology Progress, v. 27, n. 3, p. 733–743, maio 2011.

WU, H. et al. Purification and Characterization of Recombinant Human Lysozyme from Eggs of Transgenic Chickens. **PLOS ONE**, 2015.

WU, T. et al. What is new in lysozyme research and its application in food industry ? A review. **Food Chemistry**, v. 274, n. August 2018, p. 698–709, 2019.

YUJIA, L. et al. Improved antioxidant activity and physicochemical properties of curcumin by adding ovalbumin and its structural characterization. **Food Hydrocolloids**, v. 72, p. 304–311, 2017.

Thermodynamics and kinetics of curcumin-lysozyme complex formation that protects curcumin from thermal and photodegradation

Abstract

Curcumin presents many pharmacological activities such as anti-inflammatory, antimicrobial and antioxidant. However, the application of curcumin in aqueous solution is limited due to its high sensitivity to light and heat. In order to overcome these limitations, the curcumin photo and thermal protections by lysozyme were investigated at pH 7.4, using ultraviolet-visible spectrophotometry (UV-vis). The lysozyme-curcumin complex formation was confirmed by a thermodynamic analysis using surface plasmon resonance, that provided binding constants (K_b) on the order of 10^3 L mol^{-1}, with 1:1 stoichiometry. The stable complex predominated over free molecules ($\Delta G°_{298.15K}$ =−20.50 kJ mol^{-1}), being the lysozyme conformational changes the main responsible to the lysozyme-curcumin complex formation. The association of free molecules and the dissociation of the stable complex to form an intermediate complex occurred in multi-steps, being the activation energy dependent of temperature. This study shows that the formation of a complex between curcumin and lysozyme can protect curcumin from thermal and photodegradation, providing thermodynamic and kinetic data for the better application of this complex in the food, cosmetic and pharmaceutical industry.

Keywords: Curcumin, lysozyme interaction, curcumin photodegradation, curcumin thermal-degradation, thermodynamic binding, kinetic constants.

1. Introduction

Curcumin (CRC), presented in Figure 1, is a hydrophobic polyphenol isolated from the turmeric (*Curcuma longa)*, being the major active component from this plant. CRC has been used in food and chemical industries as coloring, flavoring and preservative agent (GUPTA et al., 2011; LI et al., 2015). It is well known as a natural polyphenol with a wide range of beneficial effects, such as anticancer (GUPTA et al., 2010; PRASAD; TYAGI; AGGARWAL, 2014), antiviral (MATHEW; HSU, 2018), antioxidant (YUJIA et al., 2017) and antibacterial properties (NEGI et al., 1999). Although CRC presents many medicinal benefits, its low photo and thermal stability are limiting factors for its broad industrial food application (CASTILLO et al., 2015; CHEN et al., 2014; NAKSURIYA et al., 2014).

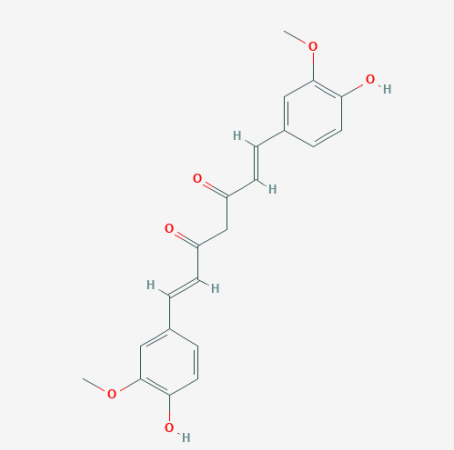

Figure 1- Chemical structure of curcumin (PubChem CID: 969516)

The use of proteins as carriers to carry CRC has received increasing interest because of their safe, biodegradable and reproducible perspective (LI et al., 2015; PAN et al., 2015). A variety of proteins has been used as CRC carriers, for instance; human serum albumin (HSA) (KUNWAR et al., 2006; MANDEVILLE; FROEHLICH; TAJMIR-RIAHI, 2009; PULLA REDDY et al., 1999), bovine serum albumin (BSA) (BOURASSA et al., 2010), β-lactoglobulin (MOHAMMADI et al., 2009; SNEHARANI et al., 2010),

casein (SAHU; KASOJU; BORA, 2008), α- lactalbumin (MOHAMMADI; MOEENI, 2015), ovalbumin (LIU et al., 2018) and lysozyme (KAMSHAD et al., 2019).

The complex formation between proteins and bioactive molecules can protect these molecules from thermal and photodegradation (Silva et al., 2018). Hen Egg White Lysozyne (LYS) has been of interest phamarceutical, cosmetics and in the food industry due to its abundance in natural resources and functional characteristics as antibacterial, antiviral and antihistamic, among others (CEGIELSKA-RADZIEJEWSKA; SZABLEWSKI, 2013; MAŁACZEWSKA et al., 2019; PARROT; NICOT, 1963b) . Moreover, this protein has a price relatively low depending on the purity level and the application required (ERCAN; DEMIRCI, 2016; WILKEN; NIKOLOV, 2011). LYS structure is composed of 129 amino acids residues, has a molecular weight of 14.3 kDa and is a basic protein (isoeletric point value of 10.7) (CAO et al., 2015; NIGEN et al., 2007) .

Some papers have reported the complex formation between LYS and CRC by fluorescence spectroscopy (FS). In a pH range between 2.0 and 7.4, it was found that the binding constant (K_b) for LYS-CRC was on the order of 10^4 M^{-1} (BORANA et al., 2014; MOHAMMADI et al., 2016; WANG; LIU; LEE, 2009). These studies bring information on the thermodynamics of the formation of the LYS-CRC complex, mainly regarding the interaction occurring near the tryptophan residues. However, as from the latest studies, there is a lack of data on the kinetics of LYS-CRC binding. This kind of study is important because, for example, the most stable complex is not always the one that forms faster and thus it is the chosen one to be used in a viable formulation (NUNES et al., 2019).

CRC decomposition generates different metabolites that leads to changes in the food sensory properties. A few papers have reported the effect of CRC complexation

on its degradation by light and temperature. It was demonstrated by high performance liquid chromatography- ultraviolet (HPLC-UV) that the complexation of CRC with γ-cyclodextrin protects CRC from the photodegradation, at room temperature (CASTILLO et al., 2015). Another work demonstrated that the $t_{1/2}$ of CRC increased 3.00 and 1.33 times after binding with native and unfolded BSA, respectively, at pH 7.0 and at 298.15K (HUDSON et al., 2018). The thermal degradation of CRC was studied, at pH 6.6 and the authors concluded that $t_{1/2}$ of complexed CRC with micellar-casein (MC) increased (compared to the $t_{1/2}$ of CRC alone) about 2.5 times at 303.15 and 313.15 K, and 1.45 times at 323.15 and 333.15 K (HUDSON et al., 2019a). All these results showed the photo and thermal protective effects of protein complexation on CRC, and, accordingly, the formation of a LYS-CRC complex could protect CRC degrading in the food matrices, as well as in agricultural and pharmaceutical products.

CRC decomposition generates different metabolites that leads to changes in the food sensory properties. A few papers have reported the effect of CRC complexation on its degradation by light and temperature. It was demonstrated that the $t_{1/2}$ of complexed CRC with micellar-casein (MC) increased, compared to the $t_{1/2}$ of CRC alone, at pH 6.6 (HUDSON et al., 2019a). Further, CRC binding with native and unfolded BSA, at pH 7.0 and at 298.15K, and the complexation of CRC with γ-cyclodextrin, at room temperature, protected CRC from the photodegradation (CASTILLO et al., 2015; HUDSON et al., 2018) . All these results showed the photo and thermal protective effects of protein complexation on CRC, and, using an easily obtainable protein and abundant in nature, the formation of a LYS-CRC complex could protect CRC degrading in the food matrices, as well as in agricultural and pharmaceutical products.

The complete thermodynamic and kinetic study of CRC binding to LYS has not been revealed, as well as the study of photo and thermal- degradation of CRC both in the absence and presence of LYS. Considering this, in this work we proposed to study the kinetics and thermodynamics of LYS-CRC complex formation using the surface plasmon resonance, and in addition, to evaluate the effect of the complex formation on the thermal and photo-degradation of CRC.

2. Material and Methods

2.1. Material

Hen egg-white lysozyme (> 90% wt) and curcumin (> 80% wt) were obtained from Sigma-Aldrich (USA), ethanol (analytical grade) from Labimpex (Brazil), dibasic sodium phosphate (Na_2HPO_4) and sodium phosphate monohydrate ($NaH_2PO_4 \cdot H_2O$) (purities 98.0%–100.0% and ≥99%, respectively) were purchased from Vetec (Brazil), and 3-(N,N-dimethylamino)propyl-N-ethylcarbodiimide (EDC) (> 99% wt), N-hydroxysuccinimide (NHS) (> 99% wt), ethanolamine-hydrochloride (> 99% wt), and sodium acetate (> 99% wt) were purchased from General Electric Healthcare Company (Uppsala, Sweden).

2.2. CRC photo and thermal degradation analysis

The photo and thermal degradation analysis were performed using a Lambda 35 UV–Vis spectrophotometer (Perkin Elmer Inc, Waltham, USA). CRC solution (2.5×10^{-5} M) was prepared with a buffer solution containing 3% of ethanol, and CRC-LYS solution was prepared from the mix of the previously prepared CRC solution with LYS, at concentration ranging from 0 to 45 μM, at room temperature and at pH 7.4.

For the photodegradation experiment, all these solutions were stored in clear glass bottles and placed into a light chamber containing two fluorescent lamps, as to

correspond to daylight. The absorbance readings at 425 nm were taken, and the absorption spectrum was obtained using a 1.0 cm quartz cells, at 298.15 K, during 2 hours, for every 10 minutes (HUDSON et al., 2018).

For the thermal degradation analyses, the CRC solutions previous described above were prepared and conditioned in the dark, in water baths of different temperatures (288.15, 293.15, 298.15 and 303.15 K). The absorbance readings at 425 nm were taken, and the absorption spectrum was obtained using a 1.0 cm quartz cells for every 6 minutes for the thermal degradation analyses (HUDSON et al., 2019a).

2.3. SPR analysis

The kinetic and thermodynamic parameters for the LYS-CRC interactions were obtained by SPR using a Biacore X100 instrument (GE Healthcare, Pittsburgh, PA, USA). Initially, LYS was immobilized on a CM5 sensor chip (GE Healthcare Company) by amine-coupling, according to the protocol recommended by the Biacore X100 handbook BR-1008-10 edition AC. This CM5 sensor chips has two flow channels: one was used as a reference surface and the other one was used for the protein immobilization.

For the immobilization of LYS on the chip surface, the CM5 chip was activated by injecting a freshly prepared mixture of EDC (0.4 M) and NHS (0.1 M) (1:1 v/v) at a flow rate of 10 μL/min for 7 min. After that, LYS (2 μg mL^{--1}) solution flowed over the sample channel of CM5 and formed covalent bonds between the amine groups of LYS and the carboxyl groups of CM5 sensor chip. The LYS solution was prepared in 10 mM sodium acetate, at a pH value of 4.0, and reacted for 7 min at a flow rate of 10 μL/min, resulting in a low-density LYS immobilization (1744 RU), which reduces any potential mass transportation (REZENDE et al., 2020). Next, the ethanolamine-hydrochloride solution at 1.0 M and at pH 8.5 flowed over the channel for 7 min to inactivate the

unreacted carboxyl groups, and so the signal (response unit, RU) was read. The flow cell used as a reference surface was prepared as described above, except for the LYS immobilization step.

The LYS-CRC binding experiments were carried out at pH 7.4, in a temperature range from 285.15 to 301.15K. The CRC solutions (10 to 70 μM) were prepared with a HBS-P buffer (0.01 M, HEPES pH 7.4, 0.15 M NaCl, 0.005% v/v Surfactant P20). The CRC solution, at a determined concentration, flowed over the two channels of the CM5 chip for 25 s. At the end of each experiment, the HBS-P buffer flowed twice, for 30 s, aiming to regenerate the chip surface and to establish the baseline.

3.0. Results and Discussion

3.1. Kinetics of the photo and thermal degradation of curcumin

It is well established that CRC has low photo and thermal stability (CHEN et al., 2014; MONDAL; GHOSH; MOULIK, 2016). For instance, exposition to light for CRC leads to degradation products, which can affect consumers health and change the color and sensory properties of foods (NADI et al., 2015; SCHNEIDER et al., 2015).

When CRC is enclosed within a hydrophobic pocket of different carriers, it is generally protected against the degradation effects of light and temperature (ARIYARATHNA; KARUNARATNE, 2016; CASTILLO et al., 2015; HUDSON et al., 2018). To evaluate the protective effect of LYS on the photodegradation of CRC we determined the kinetic photodegradation constant (K_{FD}) and the half-life time ($t_{1/2}$) of CRC in the absence and in the presence of increasing concentrations of the protein at pH 7.4. Then, the absorbance data according to the exposure time were fitted to Eq. (1) and the half-life time ($t_{1/2}$) was obtained from Eq. (2).

$$-\ln \frac{A}{A_0} = K_{FD} t \quad (1)$$

$$t_{1/2} = \frac{ln2}{K_{FD}} \quad (2)$$

where A is the absorbance at a time t, A_0 is the absorbance at the initial time and t is the storage time (h). The K_{FD} values were obtained from the slope of the plot of $-\ln A/A_0$ *versus* the time of light exposure (Figure S1).

Figure 2 shows the behavior of K_{FD} and $t_{1/2}$ parameters as a function of different LYS concentrations at temperature of 298.15 K.

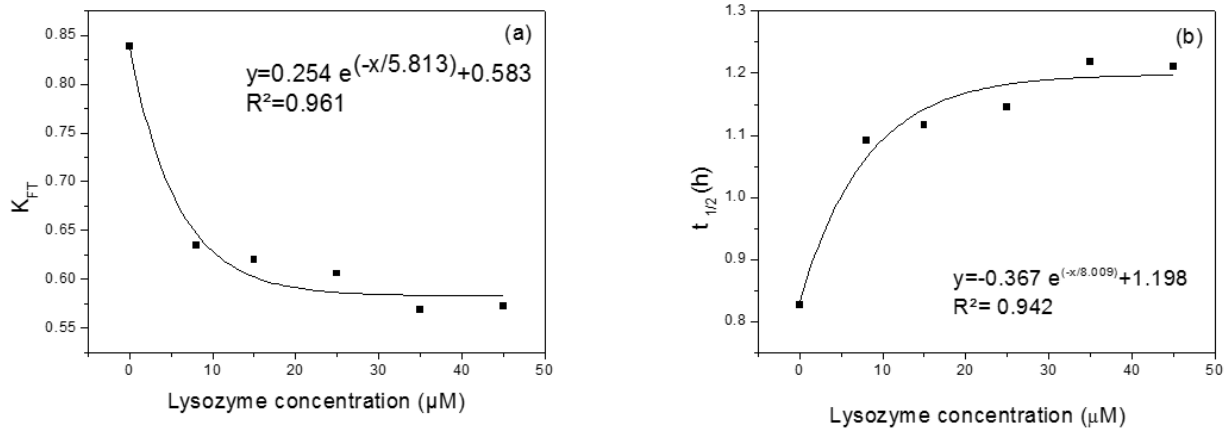

Figure 2 – Photodegradation parameters of CRC at increasing concentrations of LYS at pH 7.4 and at 298.15 K: (a) photodegradation constant (K_{FD}) and (b) half-life time ($t_{1/2}$).

As the LYS concentration increased, K_{FD} values decreased exponentially until achieving a plateau at around 35 μM of the protein, indicating that above this LYS concentration the maximum amount of CRC was complexed with the protein. Regarding the CRC $t_{1/2}$, an increasing exponential behavior was observed in the presence of increasing LYS concentrations. K_{FD} reduced 1.5 times and the $t_{1/2}$ yielded

an improvement of the same magnitude when the LYS concentration increased to 35 μM, compared with the pure CRC.

Hudson et al. (2018) investigated the protective effects of native and unfolded BSA on the light instability of CRC at pH 7.0. They found the same K_{FD} decreasing exponential behavior observed by us; however, the BSA had a stronger photo-stabilization effect on CRC, especially in its native conformation, which reduced K_{FD} in about 3.0 times and increased the $t_{1/2}$ in 2.0 times. They proposed a mechanism for the CRC photo-protection, the complex formation between CRC and native BSA, with a binding constant of 2.20×10^4 L mol^{-1}, kinetic association constant (k_a) equal to 1.49×10^4 M^{-1} s^{-1} and kinetic dissociation constant (k_d) equal to 6.77×10^{-1} s^{-1}, obtained by SPR analysis, at 298.15 K. The proposed mechanism would stabilize the structure of CRC due to CRC's interaction with BSA, making this molecule less accessible to oxygen present in the bulk, and thus preventing its photodegradation. In order to verify the mechanism of stabilization of CRC by LYS, it will be necessary to perform kinetic and thermodynamic studies of the interaction between LYS and CRC.

Kinetic analysis is a useful technique to study the thermal stability of bioactive compounds, which can have a practical application in the prediction of process rates, thermal-stability and material life-time. The kinetic thermal-degradation constant (K_{TD}) and the half-life time ($t_{1/2}$) of CRC in the presence of different LYS concentrations were determined using Eqs. (1) and (2), respectively, replacing (K_{FD}) for (K_{TD}). The (K_{TD}) values were obtained from the slope of the plot of $-\ln A/A_0$ *versus* the heat exposure time (Figure S2).

The K_{TD} and $t_{1/2}$ values of CRC at 298.15 K and at pH 7.4 are presented in Figure 3, as functions of LYS concentrations. These parameter values at 288.15,

293.15, and 303.15 K follow the same behavior and are presented in Figures S3 and S4.

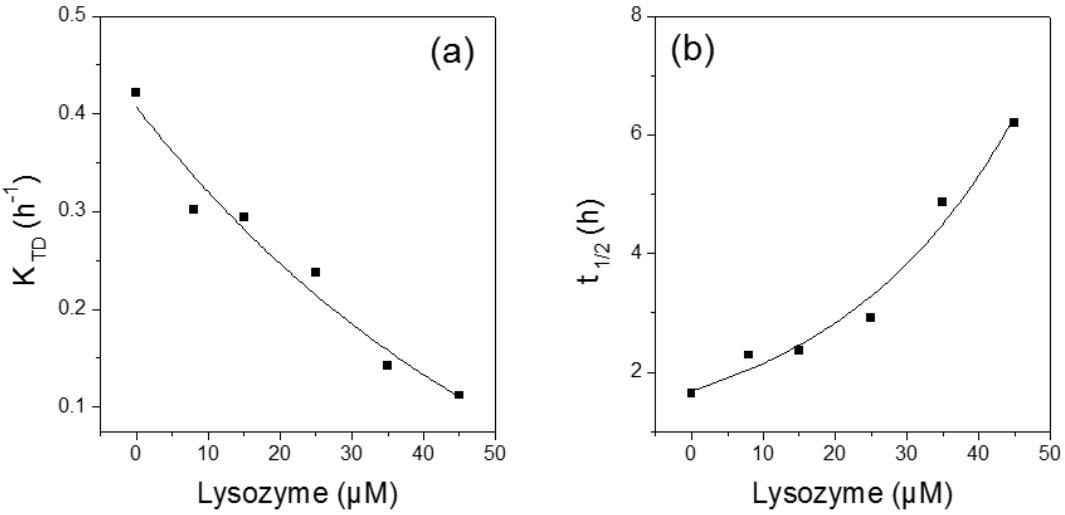

Figure 3 – Thermal-degradation parameters of CRC in the presence of increasing concentration of LYS at pH 7.4: (a) Thermal-degradation constant (K_{TD}) and (b) half-life time ($t_{1/2}$), at 298.15K

An increase in [LYS] led to an exponential reduction in the K_{TD} (mainly at 293.15 K, where K_{TD} value was 0.262 in the CRC pure solution and shifted to 0.063 after the addition of 45 μM of the protein, therefore reducing the parameter in 4.15 times and it also led to an increase on the $t_{1/2}$, for example, at 293.15 K, $t_{1/2}$ increased from 2.64 h (0 μM of the protein) to 10.96 h (45 μM of the protein), increasing at the same rate that K_{TD} was reduced. This behavior occurred to all temperatures studied, probably due to an interaction of CRC molecules with LYS, thus protecting the complex from thermal degradation.

Naksuriya et al. (2016) studied the influence of the temperature on CRC degradation at pH 8.0, in a temperature range from 310.15 to 333.15 K, using RP-

HPLC. In agreement with our results, they found that increased temperature values resulted in an increasing degradation rate for CRC.

Using the slopes of ln K_{TD} versus 1/T plots (Arrhenius plot), the activation enthalpy change of degradation ($\Delta H^{\ddagger}_{d}$) of CRC was determined using five different concentrations of LYS. Figure S5 shows the Arrhenius plots of CRC degradation, for all LYS concentrations studied, at 288.15, 293.15, 298.15 and 303.15 K.

The $\Delta H^{\ddagger}_{d}$ values express the minimal energy required for the thermal decomposition of CRC, in the presence and absence of LYS. In our study, we verified that $\Delta H^{\ddagger}_{d}$ values increased with higher LYS concentrations (Figure 4), showing that a possible complex formation leads to the stabilization of chemical bounds of CRC, protecting it from thermal degradation (HUDSON et al., 2019a).

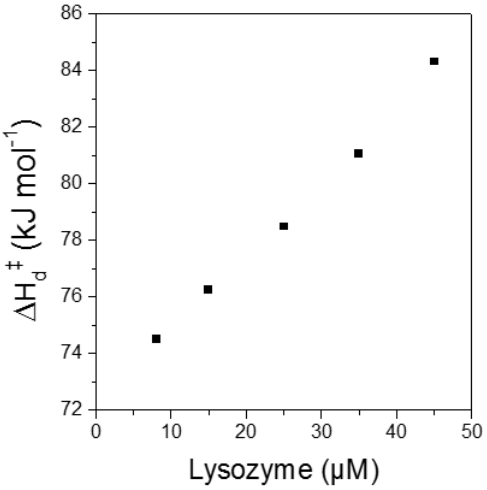

Figure 4 - Relationship of activation enthalpic energy of degradation ($\Delta H_d^{\ddagger}$) of curcumin in the presence of five different concentrations of lysozyme.

It was studied the thermal-degradation of CRC in the presence of micellar-casein, using ultraviolet-visible spectrophotometry, at pH 6.6, in a temperature range from 303.15 to 333.15 K. They found that an increase in protein concentration led to a reduction in the K_{TD} at a ratio of 3 times at 303.15 and 313.15 K and at 1.5 times at

323.15 and 333.15 K, which led to a $\Delta H_d^{\ddagger}$ of 59.76 kJ mol^{-1}. As proposed in our CRC photodegradation results, the authors proposed that CRC was protected of thermal-degradation due to its complex formation with the protein, with K_b values ranging from 3.1 x 10^3 to 11.6 x 10^3 L mol^{-1}. In addition to the thermodynamic parameters, these authors determined the kinetic energetic parameters to the activated complex formed by the association of free CRC with micellar casein, such as, the activation energy equal to - 62.8 kJ mol^{-1}, the enthalpy change of activation – 65.3 kJ mol^{-1} and the entropy change of activation -120.1 kJ mol^{-1} and, for the dissociation phase, the values of the previous parameters are 1.80 kJ mol^{-1}, 0.68 kJ mol^{-1} and -75.2 kJ mol^{-1},respectively (HUDSON et al., 2019a). Thus, reinforcing the importance of determining the kinetics and thermodynamics of the complex formation between LYS and CRC.

3.2. Study of the LYS-CRC complex formation by Surface Plasmon Resonance (SPR)

The photo- and thermal-protection of CRC in the presence of LYS suggest that LYS and CRC form a complex. The complex formation has been often studied using fluorescence spectroscopy, which is a useful tool to investigate the thermodynamics of formation of complexes between protein and bioactive molecules. However, the SPR analysis provides something else: the determination of the kinetics of the complex formation, which has not yet been studied before for LYS-CRC binding. The determination of the kinetic parameters of LYS-CRC complex formation will allow us to answer the following questions: How many LYS-CRC complexes will be formed in a second? What is the ratio of complexes dissociated at each second? What are the molecular dynamics of the complex formation?

3.2.1. Kinetics analysis of LYS-CRC binding

The kinetic parameters related to the association of LYS and CRC molecules and to the dissociation of LYS-CRC complex can be obtained by SPR analysis through the data extracted from sensorgrams (response of resonance units - RU *vs.* time). The sensorgrams for increasing concentrations of CRC flowing over the immobilized LYS at 298.15 K are presented in Figure 5.

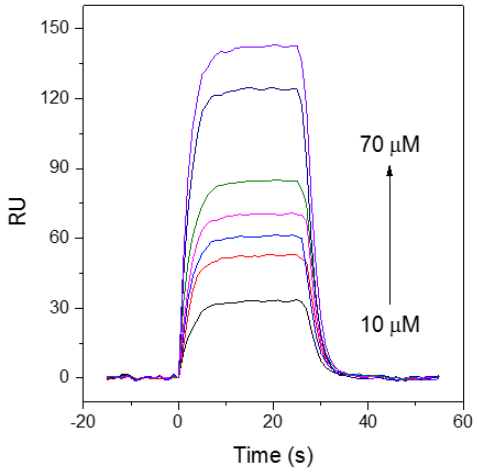

Figure 5- Sensorgrams (RU vs. Time) for LYS-CRC interaction. CRC solutions flowing over a CM5 low-density immobilized- LYS sensor-chip surface (1744 RU) at 298.15 K. The arrows indicate increasing CRC concentrations (10-70 µM).

The shape of the sensorgrams showed the changes in the RU along time, which confirmed the LYS-CRC interaction. In the baseline, between -20 to 0 s, only buffer flowed over both reference and LYS immobilized channels of the sensor chip surface, and thus, no difference in RU was observed. The RU signal showed an increasing behavior, from 0 s to 10 s, due to the fact that the buffer solution containing CRC could flow over both channels, therefore there was a predominant LYS-CRC association phenomena. After 25 s, only the buffer solution was injected again to flow over immobilized LYS, resulting in a decrease on RU and its return to the baseline, mainly

because of the dissociation of LYS-CRC. Figure S6 shows the sensorgrams obtained at the other presented temperatures (285.15, 289.15, 293.15, 297.15 and 301.15 K.).

To determine the kinetic observed (k_{obs}) and dissociation (k_d) rate constants of LYS-CRC complex formation, the global fitting of the data, at the increasing and decreasing phases of the sensorgrams, was applied and Eqs. (3) and (4) were used, respectively, based on a 1:1 molecular binding model (HUDSON et al., 2019b), which describes a simple reversible interaction of two molecules in a 1:1 complex. The kinetic association rate constant (k_a) values, which is the number of mols of LYS-CRC complexes formed per second, obtained by plotting k_{obs} *vs.* [CRC], (Eq. 5. Supplementary Figure S7) and k_d is the fraction of complexes that dissociated per second (FATHI et al., 2016). Figure 6 shows k_a and k_d behavior for the LYS-CRC interaction, at different temperatures.

$$RU\ (t) = RU_{máx}[1 - e^{-k_{obs}(t)}] \quad (3)$$

$$RU\ (t) = RU\ (t_m)\ e^{-k_d(t-t_m)} \quad (4)$$

$$k_{obs} = k_a[CRC] + k_d \quad (5)$$

where RU (t) is the SPR response at time t, $RU_{máx}$ is the maximum response of resonance unit obtained at an infinite time and RU (t_m) is the resonance unit at time t_m (s), which is the time when only the buffer flows over the CM5 chip after the CRC flow.

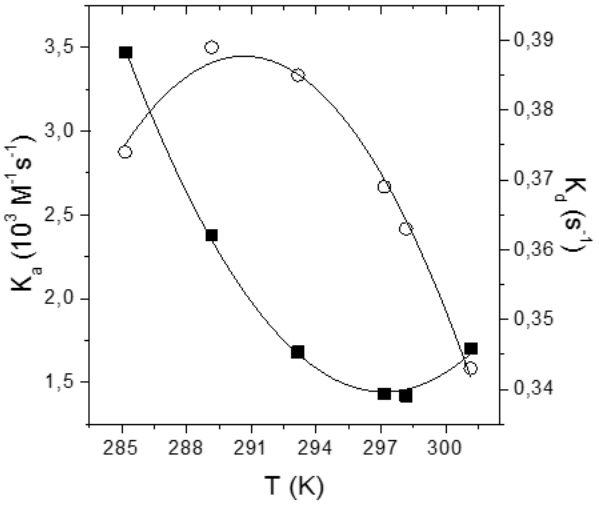

Figure 6 – Rate constants of association (k_a): (■) and of dissociation (k_d): (○) both as functions of temperature for LYS-CRC interactions. The black lines are the second order polynomial fitting for the curves, of which the determination coefficients (R^2) were 0.99 in both cases.

The k_a and k_d values showed a second-order polynomial trend. At temperatures lower than 297 K, the k_a decreased and beyond this temperature it increased with increasing temperature. Meanwhile, up to 291 K the k_d decreased with increasing temperature. Hudson et al. (2018) studied CRC binding with (BSA) at 298.15 K and found that k_a and k_d values are equal to 1.49 x 10^4 $M^{-1}s^{-1}$ and 0.677 s^{-1}, respectively. The k_a value was 10-fold higher than that one found by us at the same temperature, showing that BSA-CRC complexes are formed faster than LYS-CRC complexes. The k_d value of BSA-CRC was around 2-fold higher than what we obtained for LYS-CRC for the same temperature. These differences may be because the LYS-CRC interaction induced a stronger site fitting process than in the BSA-CRC interaction (REZENDE et al., 2019), thereby, the CRC dissociation from LYS occurs at a slower rate than CRC dissociation from BSA.

The formation of a thermodynamically stable LYS-CRC complex implies that LYS and CRC molecules should overcome an energetic barrier, and before that, an

intermediate complex is formed, usually called activated complex, from the association of free LYS and CRC molecules, or from the dissociation of the thermodynamically stable LYS-CRC complexes, Eq. (6).

$$LYS + CRC \;\rightleftarrows\; (LYS - CRC)^{*} \;\rightleftarrows\; (LYS - CRC)^{0} \tag{6}$$

where the superscript "*" and "o" indicate activated and stable LYS-CRC complexes, respectively.

Understanding the energetics of formation of the activated complex can be useful to access the dynamics of the complex formation. Using the Arrhenius plot (Figure S8) to investigate the effect of temperature on LYS-CRC binding, we obtained the activation energies involved in the association of free molecules ($E_{a(a)}$) and in the dissociation of thermodynamically stable complexes ($E_{a(d)}$) to form the activated complex. It represents the potential energy barriers related with the approximation and conformational changes in the intra and intermolecular groups in the molecules which are interacting to the formation of the activated complex. The activation energies were obtained by applying Eq. (7).

$$E_{a(y)}(T) = -R\left(\frac{d\ln K(y)}{dT}\right) \tag{7}$$

where the subscript "y" represents the association ("a") (M^{-1} s^{-1}) or dissociation ("d") (s^{-1}) phases, R (8.3145 J mol^{-1} K^{-1}) is the universal gas constant and T (K) is the temperature.

The Arrhenius plots for the association and dissociation phases showed a second order polynomial behavior, indicating that (E_{act}) values (Figure 7a) in these processes were temperature dependent, and both occurred in a multi-step induced-fit processes (ALLEN et al., 1990; NUNES et al., 2019).

Furthermore, other energetic parameters can be calculated by the temperature dependence of the k_a and k_d values. The Gibbs free energy of activation change ($\Delta G_y^{\ddagger}$),

the activation enthalpy change ($\Delta H_y^{\ddagger}$) and activation entropy change ($\Delta S_y^{\ddagger}$) related to activated complex formation can be calculated using Eqs. (8, 9 and 10). Figure 7 presents these kinetic parameters as a function of temperature.

$$\Delta G_y^{\ddagger}(T) = -RT\ ln\ \frac{k_y h}{k_B T} \quad (8)$$

$$\Delta H_y^{\ddagger}(T) = E_{a(y)}(T) - RT \quad (9)$$

$$T\Delta S_y^{\ddagger}(T) = \Delta H_y^{\ddagger}(T) - \Delta G_y^{\ddagger}(T) \quad (10)$$

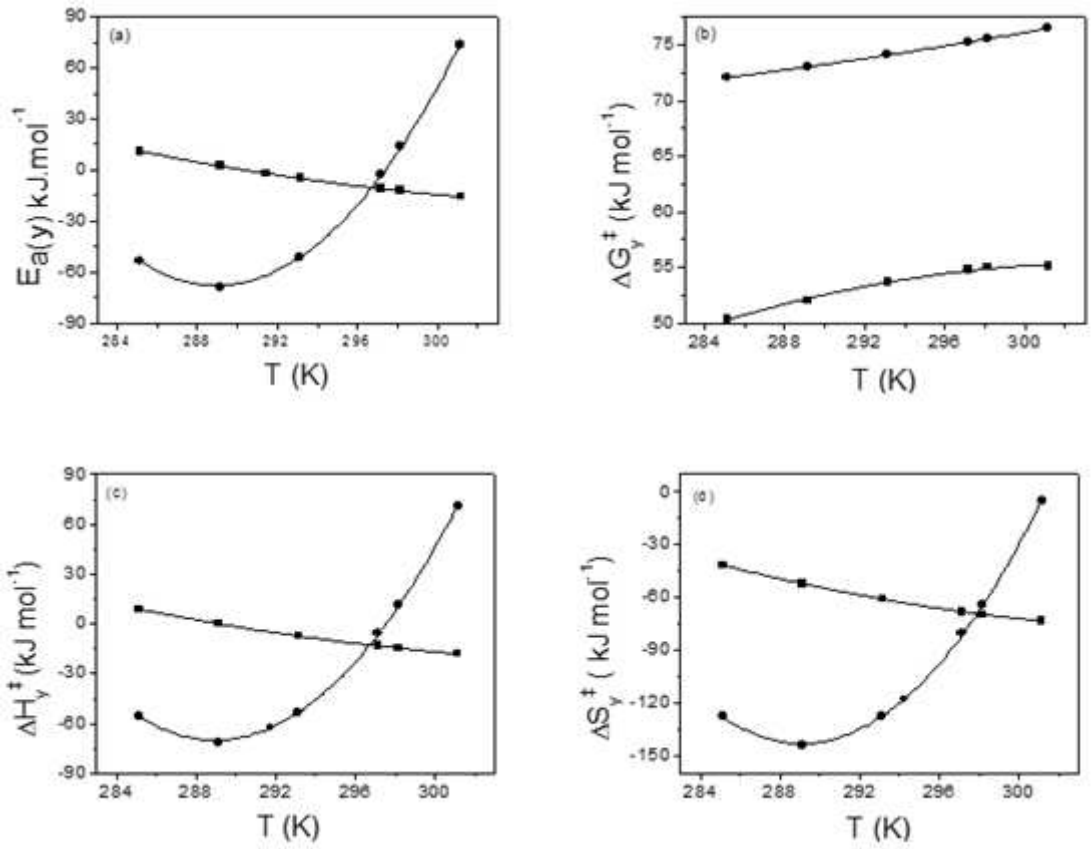

Figure 7- Energetic kinetic parameters for the formation of the activated complex by CRC with LYS association (■) and by dissociation (●) of the LYS-CRC stable complex at pH 7.4: (a) activation energy ($E_{a(y)}$), (b) Gibbs free energy of activation change ($\Delta G_y^{\ddagger}$), (c) activation enthalpy change ($\Delta H_y^{\ddagger}$), (d) activation entropy change

($\Delta S_y^{\ddagger}$). The lines are the polinomial fit, of which determination coefficients (R^2) were greater than 0.99 in all cases.

The energetic cost of ligand solvation shell and the formation/breaking of protein intra and intermolecular interactions to form the activated complex was different in the association and dissociation steps. The ($E_{a(a)}$) and ($E_{a(d)}$) presented a polynomial behavior (R^2= 0.99 for both parameters), and these energies are minimal at 314.51 K and 288.96 K, respectively.

The $\Delta G_{(\mathrm{a})}^{\ddagger}$ was lower than the $\Delta G_{(\mathrm{d})}^{\ddagger}$ values at all temperatures. Therefore, the formation of the activated complex from the association of interacting molecules occurs faster than the formation of this complex by dissociation of the thermodynamically stable complex.

To better understand the behavior of $\Delta G^{\ddagger}$ values is necessary to evaluate the contribution of the enthalpic and entropic components. The $\Delta H_a^{\ddagger}$ values showed the same behavior as $E_{a(a)}$, decreasing with increasing temperatures. The $\Delta H_a^{\ddagger}$ values can be rationalized as the contribution of three main molecular processes: the desolvation enthalpy change of the interacting molecules ($\Delta H_{(\mathrm{des})}^{\ddagger} > 0$), the energy of conformational enthalpy change of the protein-binding site induced by LYS-CRC interactions ($\Delta H_{(conf)}^{\ddagger} > 0$) and the interaction enthalpy change between CRC and the protein sites ($\Delta H_{(\mathrm{int})}^{\ddagger} < 0$). The values of $E_{a(a)}$ and $\Delta H_a^{\ddagger}$ were positive at the lowest temperature (up to 289.15 K) because the energy released by the formation of the LYS-CRC activated complex was lower than the energy required in the first and second processes.

The positive $\Delta H_a^{\ddagger}$ value can be attributed to the low flexibility in the interacting site of LYS, due to its potential rotational barrier being higher than the kinetic collisional

energy (kT). Therefore, it is necessary more energy to break intramolecular amino acid interactions when CRC reaches the binding site. Moreover, at 285.15 K, it was probably demanded more energy for releasing water to the bulk because the water molecules are more structured around the hydrophobic surface of CRC and LYS than they are at higher temperatures (NUNES et al., 2019).

Meanwhile, with the increase in temperature, the $\Delta H_a^{\ddagger}$ values decreased, showing that the energy released during the LYS-CRC interaction overcomes the energy required to the desolvation of the interacting molecules, and to conformational changes in the protein interaction sites due to the water molecules becoming less structured and thus, kT assumed the same order of the rotational barrier.

Similar to it was discussed for $\Delta H_a^{\ddagger}$, the entropic term is a result of three molecular processes: the entropy change associated with desolvation ($\Delta S_{des}^{\ddagger} > 0$), the conformational entropy change of the protein interacting site ($\Delta S_{conf}^{\ddagger}) > 0$), and the entropy change related to the complex formation ($\Delta S_{int}^{\ddagger} <0$). The entropic term ($\Delta S_{(a)}^{\ddagger}$) decreased with increased temperatures at the association phase, being the $\Delta S_{(a)}^{\ddagger}$ negative at all temperatures. So, these entropy decrease during the association of free molecules to form the activated LYS-CRC complex may be attributed to the reduction in the degree of translational freedom of both CRC and LYS molecules due to their interaction, which overcomes the entropy gain resulted from the protein conformational changes and the gain related to the release of water molecules from the solvation layer of the interacting molecules in the complex.

In the dissociation phase, $E_{a(d)}$ and $\Delta H_d^{\ddagger}$ values increased with increasing temperature, from 289.15K. These results presented an opposite behavior to that found in the association phase, showing that the molecular dynamics of formation and

breaking of LYS intramolecular interactions and solvation shell of interaction molecules are not the same during the activated complex formation from free ligands or from the dissociation of stable complexes. The main contributions involved in the conversion of the thermodynamic stable into the activated complex are the energy release caused by the interaction between LYS and CRC and the energy cost related to the conformational change of the protein-binding site. The $E_{a(d)}$ and $\Delta H_d^{\ddagger}$ values were negative at lower temperatures (up to 297.15 K) because the energy released was higher than the energy costs. However, as the temperature increased those energy costs increased and overcame the energy released by the activated complex formation, suggesting that the conformation of the protein in the activated complex, at higher temperatures, is more distinct from the protein conformation in the stable complex. The entropy values ($\Delta S_{(d)}^{\ddagger}$) also increased with increasing temperatures. This indicates that the gain in the conformational entropy of the LYS interacting site and the desolvation entropy of the stable complex were higher than the reduction in the entropy of the system caused due to the formation of the active complex.

3.2.2. Thermodynamic analysis

The SPR data also allow us to know about the thermodynamic of LYS-CRC complex formation. While the kinetic parameters provide information about the association and dissociation speed of the stable complexes and about the molecular dynamics of complex formation, the thermodynamic parameters contribute to better understand the driving forces involved in the complex formation process. Thereby, kinetic and thermodynamic characterization are complementary, being important in the effective application of complexes between protein and bioactive molecules in foods and other matrices (NUNES et al., 2019).

The binding constant (K_b), at each temperature, was calculated according to the relationship: $K_b = K_a/K_d$, then the standard Gibbs free energy change (ΔG°) values were obtained from K_b values using Eq. (11). The thermodynamic parameters for LYS-CRC complex formation are shown in Table 1.

$$\Delta G° = -RTlnk_b \quad (11)$$

Table 1- The binding constant (K_b), standard changes in Gibbs free energy (ΔG°), enthalpy (ΔH°), and entropy (TΔS°) for the LYS-CRC complex formation at different temperatures (T) and pH 7.4. Data obtained from SPR measurements.

Temperature	K_b	ΔH°	ΔG°	TΔS°	ΔCp°
(K)	(10^3 M^{-1})		(kJ.mol^{-1})		kJ.mol^{-1}.K^{-1}
285.15	9.28	-64.61	-21.66	-42.96	-4.93
289.15	6.12	-71.39	-20.96	-50.43	2.37
293.15	4.36	-46.41	-20.43	-25.99	9.68
297.15	3.88	7.78	-20.41	28.19	16.99
298.15	3.91	25.61	-20.50	46.11	18.81
301.15	4.96	88.84	-21.30	110.14	24.29

The K_b values followed a second-order polynomial behavior as a function of temperature (y= 3.85 x 10^6 - 2.59 x 10^4 X + 43.78 X^2, R^2 = 0.998), and they were of the order of 10^3 M^{-1}. At 285.15K are former more LYS-CRC complexes than in the other studied temperatures.

The LYS-CRC interaction has been studied by FS, at different concentrations, pH and temperature range. Wang et al. (2009) studied LYS-CRC interactions from 283.15 to 328.15 K, at pH 2.0 and obtained K_b values of the order of 10^4 M^{-1}. Borana et al. (2014) also studied these interactions at room temperature, pH 7.4 and they obtained K_b of the order of 10^4 M^{-1}. Li et al. (2015) studied the same system at pH 7.0 and they obtained K_b = 9.8x10^3 M^{-1}, at 298.15 K. Mohammadi et al. (2016) studied the

system formed by LYS and CRC at pH 6.4; from 293.15 to 303.15 K, and they obtained K_b of the order of 10^4 M^{-1}. The K_b values determined in our SPR study were from 2.5 up to 10 times smaller than the K_b values determined by the other studies. This can be explained by the different techniques used in these studies (Paula et al., 2017). Fluorescence spectroscopy can only detect interactions that occur directly with fluorophore-labeled residues, in this case, the interactions with the sites close to tryptophan (Trp) residues while SPR can detect the interactions occurring in all the LYS sites. So, each interaction site has its own interaction constant (K_b), and this value is a weighted average of K_b in each site of interaction ($K_{b,i}$), Eq. (12) (HUDSON et al., 2019a) .

$$K_B = \frac{\sum n_i k_{B,i}}{n_t} \quad (12)$$

where n_i is the number of LYS sites with interaction constants and n_t is the total number of sites present in a LYS.

Hence, the difference in the order of the K_b values obtained by SPR and those obtained from the literature were probably due to the interactions occurring in the in the LYS sites not close to the Trp residues, which could be noticed only by the SPR technique.

The plot between (ln K_b) vs. (1000/T) (Figure 8) showed a second-order polynomial behavior, so, the values of standard enthalpy change (ΔH°) were calculated using nonlinear Van't Hoff approach, where the ΔH° values can be determined by the tangent of the curve at any point along the curve. The dependence of ln K_b on T can be approximated by a polynomial expression using Eq. (13) (SILVA et al., 2008; VIEIRA; BASSO; COSTA-FILHO, 2017). The values of the constants a, b, c and d were obtained from this plot, using a least-squares regression procedure.

$$lnk_B = a + \frac{b}{T} + \frac{c}{T^2} + \frac{d}{T^3} + \cdots \quad (13)$$

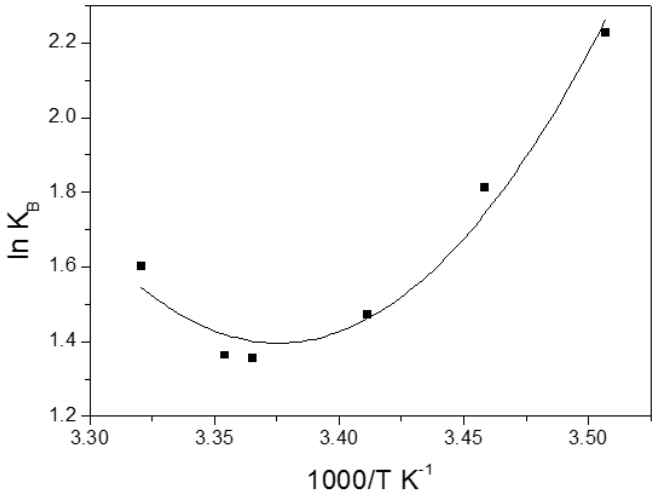

Figure 8- Plot of ln K_b (■), obtained by SPR, as functions of reciprocal temperature.

Finally, the enthalpic and entropic contributions to $\Delta G°$ (ΔH° and TΔS°) were calculated using Eqs. (14) and (15), respectively.

$$\Delta H° = -R\left(b + \frac{2c}{T} + \frac{3d}{T^2}\right) \quad (14)$$

$$\Delta G° = \Delta H° - T\Delta S° \quad (15)$$

where R is the universal gas constant (8.3145 J mol^{-1} K^{-1}), T is the temperature (K), ΔH° is the standard enthalpy change (kJ mol^{-1}), ΔG° is the standard Gibbs free energy change (kJ mol^{-1}), and ΔS° is the standard entropy change (kJ mol^{-1} K^{-1}).

All $\Delta G°$ values were negative, showing that at chemical equilibrium (LYS + CRC ⇋ LYS-CRC) the concentration of LYS-CRC complex was higher than the concentration of LYS and CRC molecules, being the complexes more stable at 285.15 K. The values of the enthalpic and entropic terms increased with increasing temperatures. We must consider that the $\Delta H°$ and $T\Delta S°$ values are influenced by the

same three molecular processes previously discussed to explain the behavior of $\Delta H^{\ddagger}$ and $T\Delta S^{\ddagger}$ parameters.

At lower temperature, the enthalpic values are negative, because the energy released due to the interaction between CRC and protein interaction sites outweighs two process: the energy necessary to desolvation of the interacting molecules and the energy necessary to conformational changes of the protein-binding site, showing that the process is exothermic and enthalpically driven at lower temperature. This negative value can be due two reasons: i) at low temperature, the average kinetic energy is lower than rotational barrier energy or ii) the structuration degree of water molecules present in bulk is almost the same that those present in solvation layer at low temperature. Thus, the energy released from the interaction between LYS and CRC when the LYS-CRC complex is formed dominates and the ΔH° value is negative at low temperature (WANG; CHEN; ZHANG, 2010). However, as the temperature increases, the energetic cost spent to change the conformation of the protein when it interacts with CRC is smaller, since the average kT at high temperature is higher than the rotational barrier of conformational changes. In addition, at high temperatures, the water molecules released from solvation layer are in higher degree of disruption in the bulk, which also contributes the large increase in the enthalpy and entropy values up to 296.70 K, suggesting that hydrophobic interaction may played a major role in the binding process at higher temperature, contributing remarkably to the stability of the LYS-CRC complex.

Wang et al. (2009) studied the thermodynamic of LYS-CRC system by fluorescence spectroscopy, at pH 2.0 and a range of temperature from 283.15 to 328.15 K, using four temperatures. They used a linear Van't Hoff approach to analyze their data, and they obtained only one value of enthalpy (ΔH = -78.39 kJ/mol) and

entropy change (TΔS = -0.17 kJ / mol. K). Mohammadi et al. (2016) studied the same system by the same technique, at pH 6.4, from 293 to 303 K, using three temperatures. As the previous study, they obtained the thermodynamic parameters by the Van't Hoff equation, and there was found a single value of enthalpy (ΔH = - 59.00 kJ/mol) and entropy change (TΔS = - 0.12 kJ / mol. K). Both studies showed that the LYS-CRC interaction is enthalpically driven and exothermic, at these conditions.

The Van't Hoff linear approach consider that the enthalpy values are constant for all temperatures, therefore, the previous works only found a unique behavior for all temperature studied. Meanwhile, in our study, performed using six temperature values, we found a second-order polynomial behavior to K_b values, and consequently, the dependence of ln K_b on temperature reciprocal should be consider, using the non-linear Van't Hoff approach to extract more reliable estimates of ΔH° values (Silva et al., 2008).

It is interesting to observe that while the ΔH° and TΔS° values have remarkable changed along temperature, the ΔG° has almost maintained constant, suggesting the occurrence of enthalpy-entropy compensation (EEC). Thus, the relation between entropy and enthalpy was further investigated. Figure 9 (a) illustrates the plot of ΔH° *vs.* TΔS°.

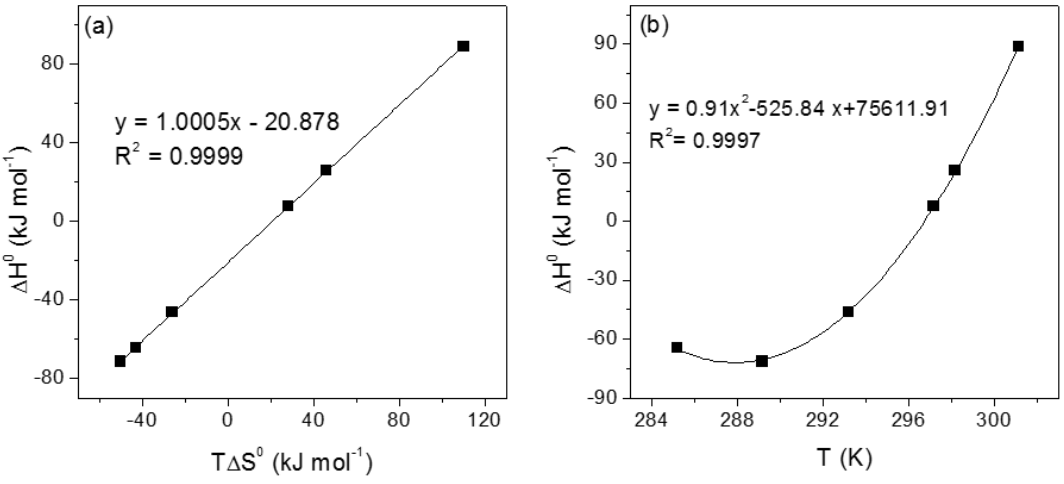

Figure 9 – (a) Changes in enthalpy (ΔH°) as functions of entropic term (TΔS°) for LYS-CRC interaction at pH 7.4. (b) Changes in enthalpy (ΔH°) as functions of temperature.

The EEC is an important phenomenon involved in various processes of biomolecules interaction (APARICIO-RUIZ; MÍNGUEZ-MOSQUERA; GANDUL-ROJAS, 2011; CHEN; LIN; HUANG, 1998; COELHO et al., 2019) . It is characterized by $\Delta\Delta G^{\circ} \approx 0$ and $\Delta\Delta H^{\circ} \approx T\Delta\Delta S^{\circ}$ (PAIVA et al., 2020). Analyzing Fig. 9a, the slope of the plot was near a unit (α=1.0005), probing that the increasing in the TΔS° values was accomplished by a proportional increasing in the ΔH° values. The water molecules of solvation layer play an important role in the EEC (FOX et al., 2018) . The increase in the entropy is owing to the release of water from the solvation layer of both interacting molecules (LYS and CRC). However, the enthalpy also increases, compensating the increasing in the entropy, because of energy absorption due to breaking of interactions between water molecules.

Up to now, our results showed that conformational changes and desolvation may play important roles in the LYS-CRC complex formation. In order to gain more insights on the energy and structural changes that occurs due to LYS-CRC interaction, we used the Eq. (16) to determine the standard heat capacity change (ΔC_p^o) (Figure 9b, Table 1). The ΔC_p^o values may help us to understand which is the main contribution to the LYS-CRC complex formation: the LYS conformation changes or the water molecules desolvation.

$$\Delta C_p^0 = \left(\frac{\partial H^0}{\partial T}\right)_P \tag{16}$$

where ΔC_p^0 is the standard heat capacity change, $\left(\frac{\partial H^0}{\partial T}\right)_P$ is the partial derivate of the standard enthalpy change, at constant pressure.

Considering that $\Delta C_p^o = C_{p\,LYS-CUR}^o - (C_{p-LYS}^o + C_{p-CUR}^o)$, the negative ΔC_p^o at the smaller temperature (285.15 K) indicates that the LYS-CRC complex was formed with weaker interactions than those existing in the free LYS and CRC molecules. As we previously observed, ΔH° and TΔS° values were negative at low temperature, suggesting that there is no contribution of desolvation of water molecules. Hence, the negative ΔCp° value at low temperature is owing to the conformational change in the LYS binding site that, when the LYS-CRC complex is formed, forms weaker interactions than those existing between amino acids before the complex formation.

However, as the temperature increased, the ΔC_p^o became increasingly positive, showing that the LYS-CRC complex possesses stronger interactions than the free reactants. This result can also be explained by the conformational changes that occurred in the binding site of the protein during the LYS-CRC complex formation. We believe that when the CRC enters the binding site of LYS, its conformation becomes more structured, i.e., stronger interactions (than those previously existing between amino acids) are formed. Therefore, by the analysis of ΔCp°, we can conclude that conformational changes are the main responsible for the complex formation between LYS and CRC. In agreement with our results, a LYS-CRC interaction study found by CD spectroscopy that the secondary structure of LYS changed in presence of CRC. The percentage of LYS α-helix decreased, suggesting an unfolding of LYS structure during the binding to CRC, hence, indicating protein conformational changes during this interaction (KAMSHAD et al., 2019).

4.0. Conclusions

The study of photo and thermal degradation of CRC revealed that the interaction between LYS and CRC can protect this bioactive molecule, due to the complex formation between those two molecules. The SPR thermodynamic study confirmed the LYS-CRC complex formation, at pH 7.4. This complex formation was enthalpically driven up to 293.15 K and entropically driven after 297.15 K. Furthermore, we found, after using six different temperatures that the dependence of ln with the temperature parameter should be considered, using the non-linear Van't Hoff approach, applied for the first time for the LIS-CRC binding, to extract more reliable estimates of ΔH°, allowing us to conclude by the analysis of ΔCp° that LYS conformational changes are the main responsible for the complex formation between LYS and CRC. The kinetics study revealed that the formation of the activated complex from the association of interacting molecules occurs faster than the formation of this complex by dissociation of the thermodynamically stable complex. Besides, it was also demonstrated that the activated complex formation during association or the dissociation phase occurred in a multi-step process, being temperature dependent.

Based on these results, LYS may be used to improve the photo and thermal stability of CRC; and, the information about the kinetics and thermodynamic of this complex shall be useful for the successful application of this bioactive molecule in the food, cosmetic and pharmaceutical industry.

Acknowledgments

This work was supported by the Conselho Nacional de Desenvolvimento Científico e Tecnológico (CNPq); the Coordenação de Aperfeiçoamento de Pessoal de Nível Superior (CAPES) and the Fundação de Amparo à Pesquisa do Estado de Minas Gerais (FAPEMIG).

Supplementary data

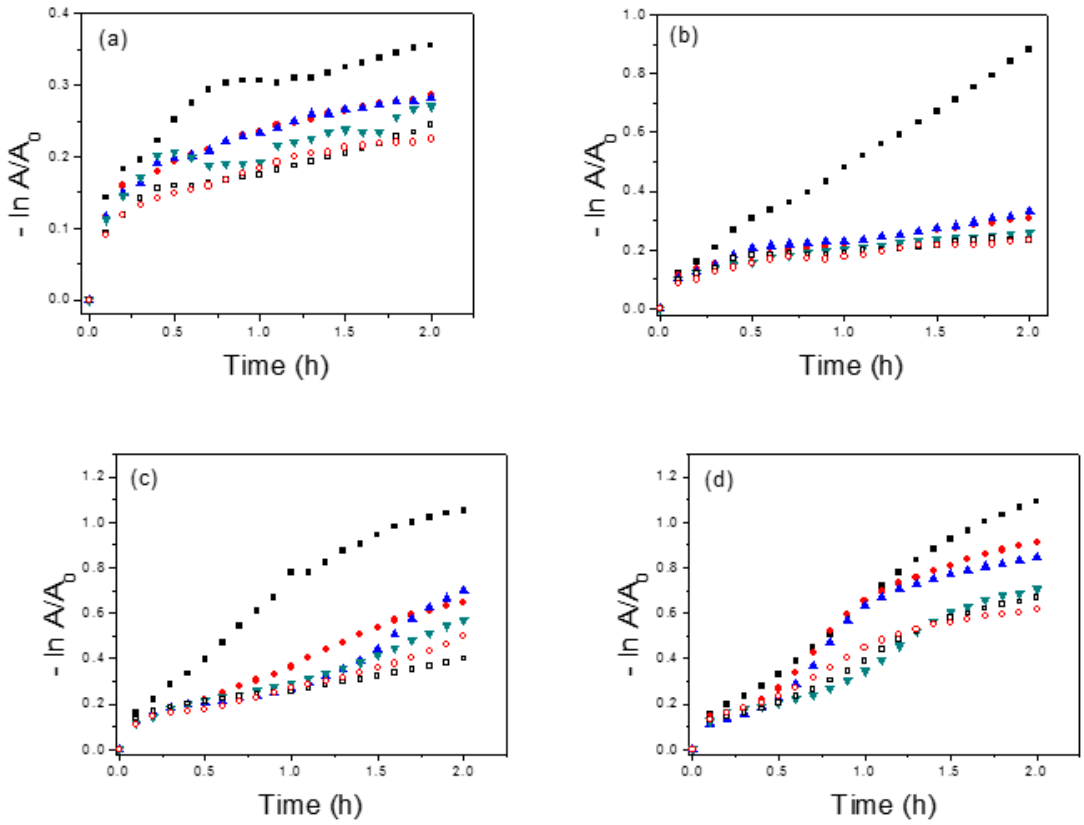

Figure S1- Plot of −ln A/A_0 versus the time of light exposure, used to obtain K_{FD} values: (a) at 288.15 K, (b) at 293.15 K, (c) at 298.15K and (d) at 303,15K. The K_{FD} of curcumin were obtained in the presence of the following concentrations of lysozyme: (■) 0 μM; (●) 8 μM; (▲) 15 μM; (▼) 25 μM; (□) 35 μM; and (○) 45 μM.

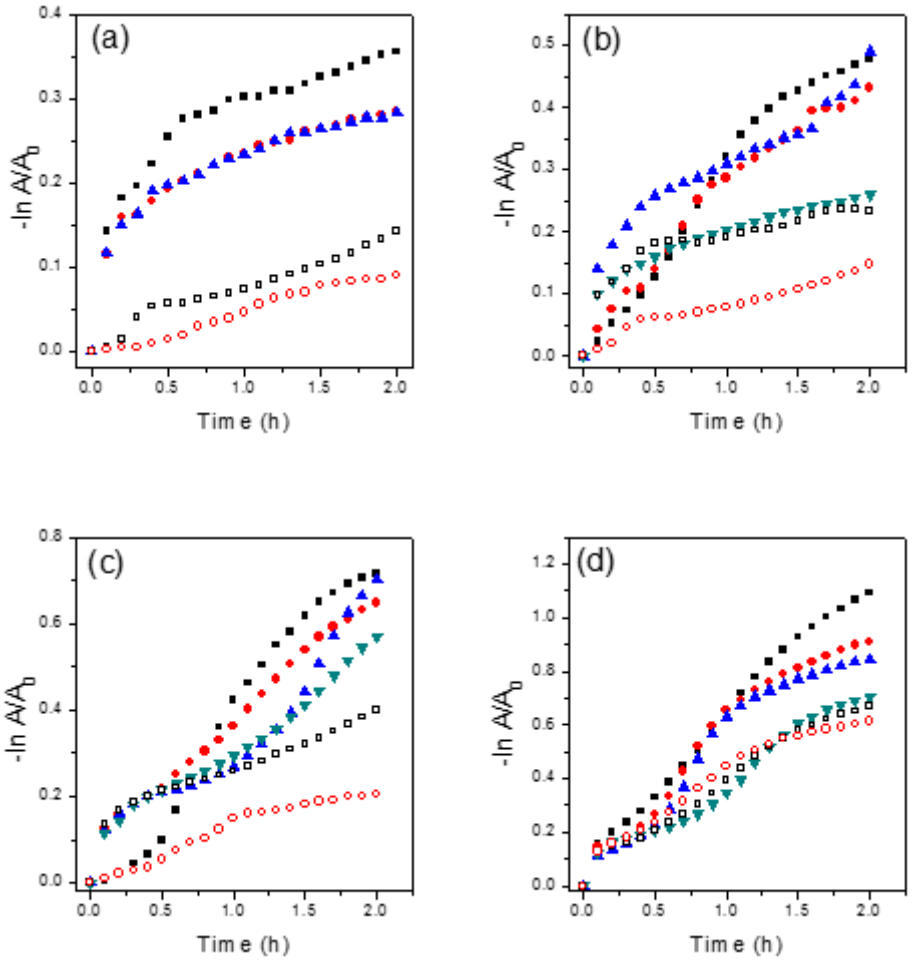

Figure S2- Plot of −ln A/A_0 *versus* the heat exposure time for obtaining the kinetic thermal-degradation constants (K_{TD}) at pH 7.4, and at temperatures: (a) at 288.15 K, (b) at 293.15 K, (c) at 298.15K and (d) at 303,15K. The K_{TD} of CRC were obtained in the presence of the following concentrations of lysozyme: (■) 0 μM; (●) 8 μM; (▲) 15 μM; (▼) 25 μM; (□) 35 μM; and (○) 45 μM.

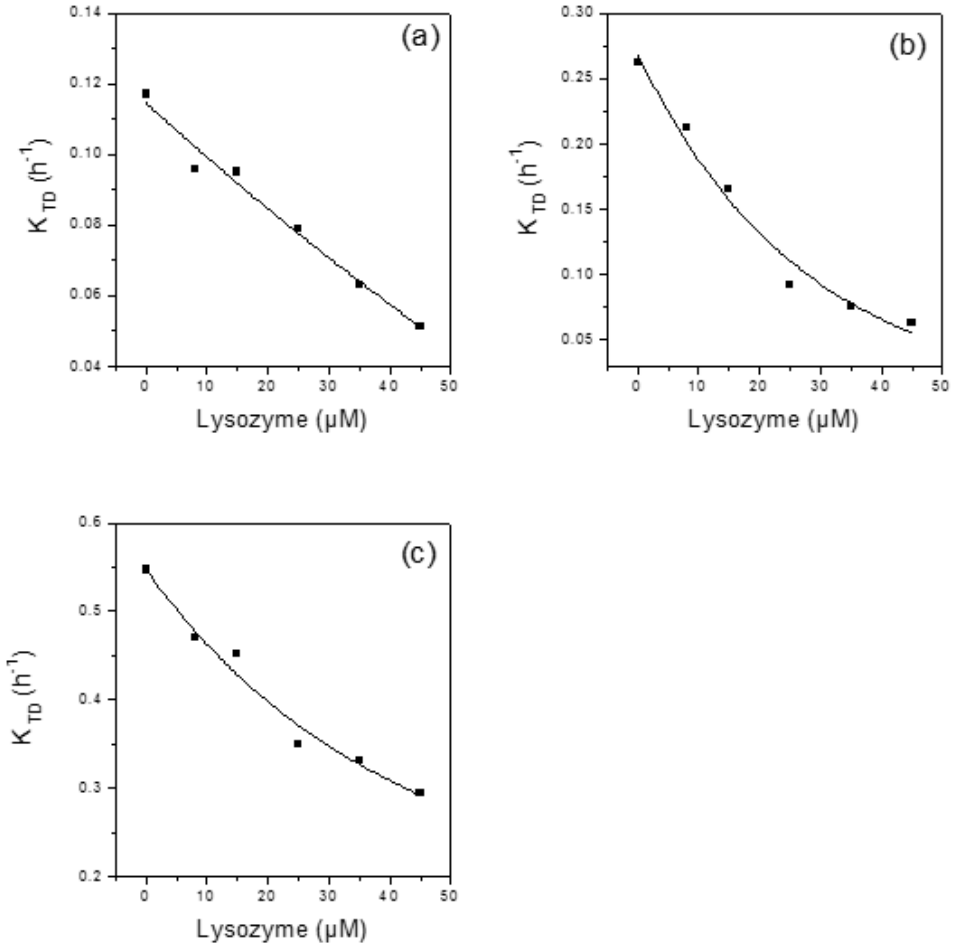

Figure S3- Kinetic thermal degradation constant (K_{TD}) of CRC as a function of LYS concentration at (a) 288.15 K, (b) 293.15 K, and (c) 303.15 K, at pH 7.4.

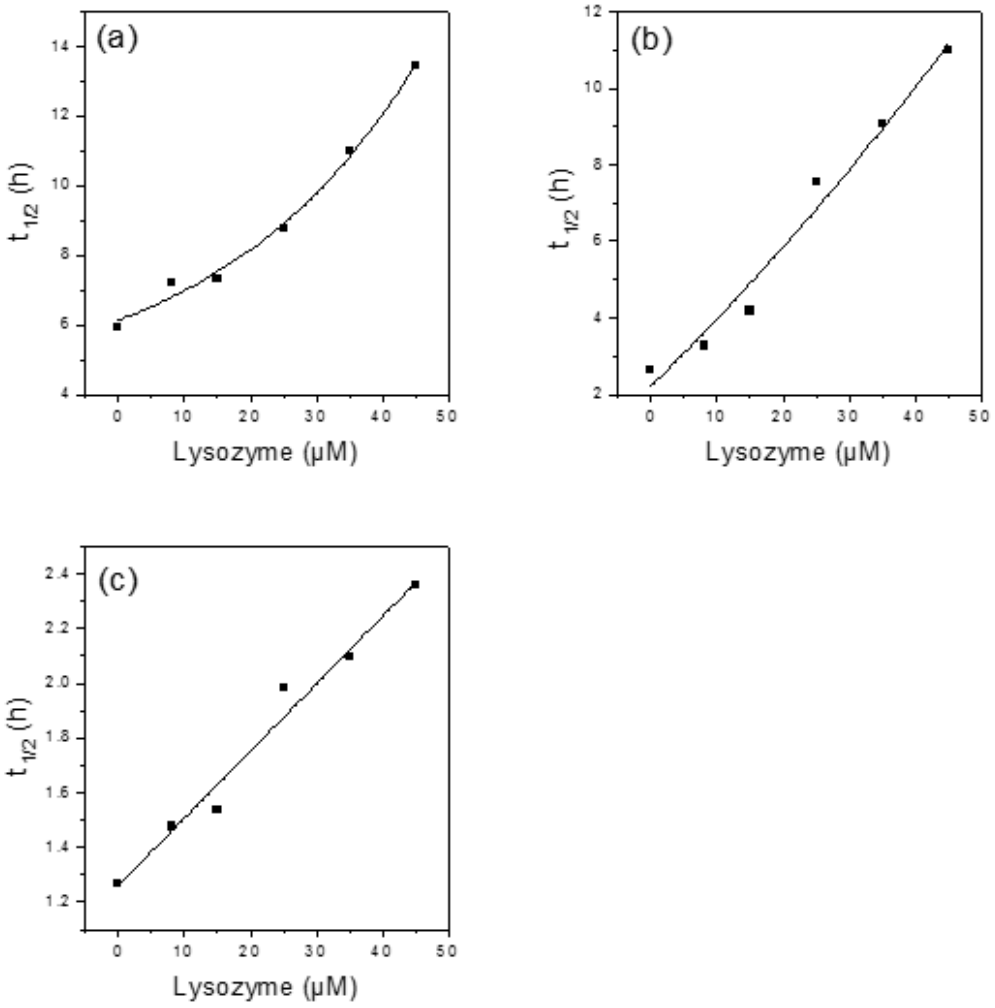

Figure S4- The half-life ($t_{1/2}$) of CRC as a function of LYS concentration at (a) 288.15 K, (b) 293.15 K, and (c) 303.15 K, at pH 7.4.

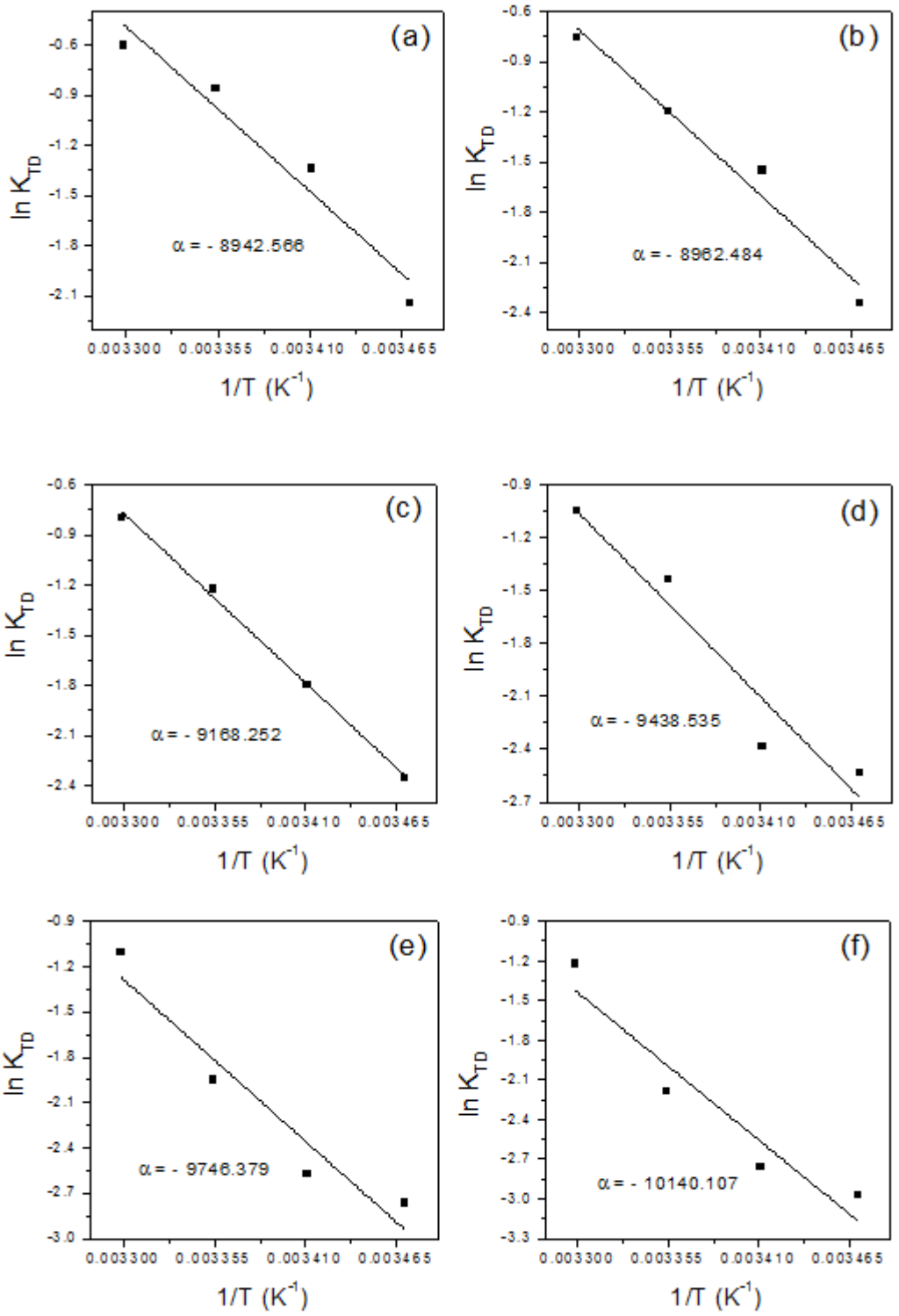

Figure S5 - Arrhenius plot of curcumin degradation in the presence of (a) 0 µM; (b) 8 µM; (c) 15 µM; (d) 25 µM; (e) 35 µM; and (f) 45 µM of lysozyme, at 288.15 K; 293.15 K; 298.15 K; and 303.15 K temperatures and pH 7.4.

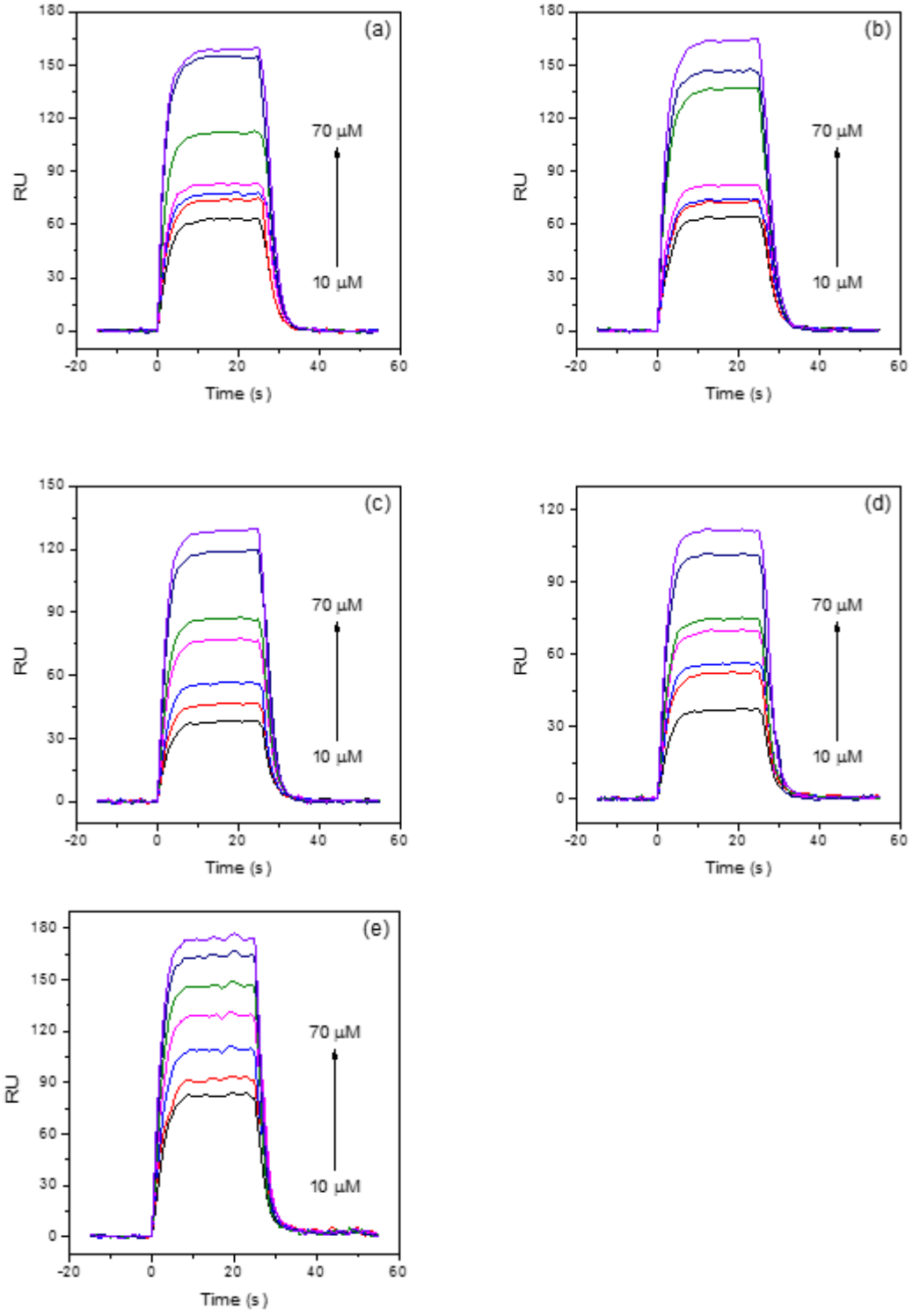

Figure S6. Sensograms (RU vs. Time) for LYS-CRC binding. 10-70 µM of CRC solutions flowing over a CM5 low-density LYS - immobilized sensor-chip surface (1744 RU): (a) 285.15 K, (b) 289.15 K, (c) 293.15 K, (d) 297.15 K and (e) 301.15 K.

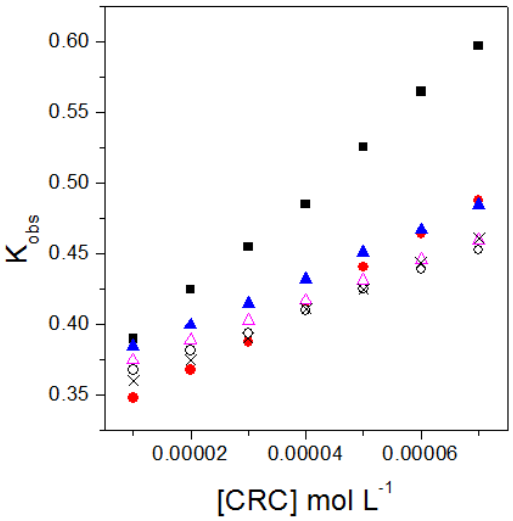

Figure S7. Plot of K_{obs} as a function of CRC concentration, used to determine k_a at temperatures: (■) 285.15 K, (●) 289.15 K, (▲) 293.15 K, (○) 297.15 K, (Δ) 298.15 K and (X) 301. 15 K.

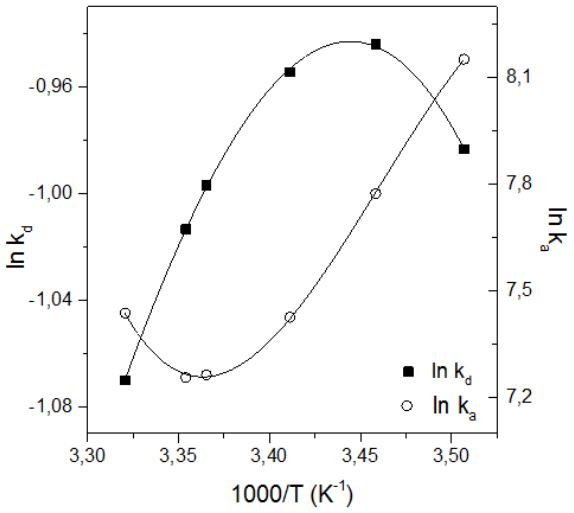

Figure S8-Arrhenius plots of ln ka (■) and ln kd (○) associated with LYS-CRC interactions as functions of reciprocal temperature, at pH 7.4.

5.0 References

ALLEN, B. et al. A Ligand-induced , Change in Penicillopepsin. **The Journal of Biological Chemistry**, v. 265, n. 9, p. 5060–5065, 1990.

APARICIO-RUIZ, R.; MÍNGUEZ-MOSQUERA, M. I.; GANDUL-ROJAS, B. Thermal degradation kinetics of lutein, β-carotene and β-cryptoxanthin in virgin olive oils. **Journal of Food Composition and Analysis**, v. 24, n. 6, p. 811–820, set. 2011.

ARIYARATHNA, I. R.; KARUNARATNE, D. N. Microencapsulation stabilizes curcumin for efficient delivery in food applications. **Food Packaging and Shelf Life**, v. 10, p. 79–86, dez. 2016.

BORANA, M. S. et al. Curcumin and kaempferol prevent lysozyme fibril formation by modulating aggregation kinetic parameters. **Biochimica et Biophysica Acta - Proteins and Proteomics**, v. 1844, n. 3, p. 670–680, 2014.

BOURASSA, P. et al. Resveratrol , Genistein , and Curcumin Bind Bovine Serum Albumin †. **Journal of Physical Chemistry B**, v. 114, p. 3348–3354, 2010.

CALLEWAERT, L.; MICHIELS, C. W. Lysozymes in the animal kingdom. **Journal of Biosciences**, v. 35, n. 1, p. 127–160, 23 mar. 2010.

CAO, D. et al. Expression of Recombinant Human Lysozyme in Egg Whites of Transgenic Hens. **PLOS ONE**, v. 10, n. February 2015, p. 1–15, 2015.

CASTILLO, M. L. R. DEL et al. Stabilization of curcumin against photodegradation by encapsulation in gamma-cyclodextrin: A study based on chromatographic and spectroscopic (Raman and UV–visible) data. **Vibrational Spectroscopy**, v. 81, p. 106–111, nov. 2015.

CEGIELSKA-RADZIEJEWSKA, R.; SZABLEWSKI, T. Effect of Modified Lysozyme on the Microflora and Sensory Attributes of Ground Pork. **Journal of Food**

Protection, v. 76, n. 2, p. 338–342, 2013.

CHEN, L. J.; LIN, S. Y.; HUANG, C. C. Effect of hydrophobic chain length of surfactants on enthalpy-entropy compensation of micellization. **Journal of Physical Chemistry B**, v. 102, n. 22, p. 4350–4356, 28 maio 1998.

CHEN, Z. et al. Thermal degradation kinetics study of curcumin with nonlinear methods. **Food Chemistry**, v. 155, p. 81–86, jul. 2014.

CHENG, Z. Studies on the interaction between scopoletin and two serum albumins by spectroscopic methods. **Journal of Luminescence**, v. 132, p. 2719–2729, 2012.

COELHO, Y. L. et al. Lactoferrin-phenothiazine dye interactions: Thermodynamic and kinetic approach. **International Journal of Biological Macromolecules**, v. 136, p. 559–569, 1 set. 2019.

DAS, S. et al. Binding of naringin and naringenin with hen egg white lysozyme: A spectroscopic investigation and molecular docking study. **Spectrochimica Acta - Part A: Molecular and Biomolecular Spectroscopy**, v. 192, p. 211–221, 2017.

DAY, E. S. et al. Determining the affinity and stoichiometry of interactions between unmodified proteins in solution using Biacore. **Analytical Biochemistry Journal**, v. 440, p. 96–107, 2013.

DE PAULA, H. M. C. et al. Kinetics and thermodynamics of bovine serum albumin interactions with Congo red dye. **Colloids and Surfaces B: Biointerfaces**, v. 159, n. 2017, p. 737–742, 2017.

ERCAN, D.; DEMIRCI, A. **Recent advances for the production and recovery methods of lysozymeCritical Reviews in Biotechnology**Taylor and Francis Ltd, , 1 nov. 2016.

FATHI, F. et al. Kinetic studies of bovine serum albumin interaction with PG

and TBHQ using surface plasmon resonance. **International Journal of Biological Macromolecules**, v. 91, p. 1045–1050, out. 2016.

FOX, J. M. et al. The Molecular Origin of Enthalpy/Entropy Compensation in Biomolecular Recognition. **Annual Review of Biophysics**, v. 47, n. 1, p. 223–250, 2018.

GHAYOUR, N. et al. Nanoencapsulation of quercetin and curcumin in casein-based delivery systems. **Food Hydrocolloids**, v. 87, n. March 2018, p. 394–403, 2019.

GHOSH, R.; CUI, Z. F. Purification of Lysozyme Using Ultrafiltration. **Biotechnology and Bioengineering**, v. 68, p. 191–203, 2000.

GUPTA, S. C. et al. **Regulation of survival, proliferation, invasion, angiogenesis, and metastasis of tumor cells through modulation of inflammatory pathways by nutraceuticalsCancer and Metastasis Reviews**, set. 2010.

GUPTA, S. C. et al. Multitargeting by curcumin as revealed by molecular interaction studies. **Natural Product Reports - Royal Society of Chemistry**, v. 28, p. 1937–1955, 2011.

HEGDE, A. H.; SANDHYA, B.; SEETHARAMAPPA, J. Investigations to reveal the nature of interactions of human hemoglobin with curcumin using optical techniques &. **International Journal of Biological Macromolecules**, v. 52, n. January 2012, p. 133–138, 2013.

HUDSON, E. A. et al. Thermodynamic and kinetic analyses of curcumin and bovine serum albumin binding. **Food Chemistry**, v. 242, n. August 2017, p. 505–512, 2018.

HUDSON, E. A. et al. Curcumin micellar-casein multisite interactions

elucidated by surface plasmon resonance. **International Journal of Biological Macromolecules**, v. 133, n. July 2019, p. 860–866, 2019a.

HUDSON, E. A. et al. Energetic parameters of β-casein/quercetin activated and thermodynamically stable complex formation accessed by Surface Plasmon Resonance. **Colloids and Surfaces B: Biointerfaces**, v. 181, n. June, p. 798–805, 2019b.

IMOTO, T. et al. Fluorescence of Lysozyme : Emissions from Tryptophan Residues 62 and 108 and Energy Migration. **Proceedings of the National Academy of Sciences of the United States of America**, v. 69, n. 5, p. 1151–1155, 1971.

JAGANNATHAN, R.; ABRAHAM, P. M.; PODDAR, P. Temperature-dependent spectroscopic evidences of curcumin in aqueous medium: A mechanistic study of its solubility and stability. **Journal of Physical Chemistry B**, v. 116, n. 50, p. 14533–14540, 2012.

KAMSHAD, M. et al. Use of spectroscopic and zeta potential techniques to study the interaction between lysozyme and curcumin in the presence of silver nanoparticles at different sizes. **Journal of Biomolecular Structure and Dynamics**, v. 37, n. 8, p. 2030–2040, 2019.

KUNWAR, A. et al. Transport of liposomal and albumin loaded curcumin to living cells: An absorption and fluorescence spectroscopic study. **Biochimica et Biophysica Acta - General Subjects**, v. 1760, n. 10, p. 1513–1520, out. 2006.

LESNIEROWSKI, G.; STANGIERSKI, J. Trends in Food Science & Technology What ' s new in chicken egg research and technology for human health promotion ? - A review. **Trends in Food Science & Technology**, v. 71, n. June 2016, p. 46–51, 2018a.

LESNIEROWSKI, G.; STANGIERSKI, J. What's new in chicken egg research

and technology for human health promotion? - A review. **Trends in Food Science and Technology**, v. 71, n. October 2017, p. 46–51, 2018b.

LI, Z. et al. Curcumin encapsulated in the complex of lysozyme / carboxymethylcellulose and implications for the antioxidant activity of curcumin. **Food Research International**, v. 75, p. 98–105, 2015.

LIU, X. et al. Investigation of the interaction for three Citrus flavonoids and α - amylase by surface plasmon resonance. **Food Research International**, v. 97, p. 1–6, 2017a.

LIU, Y. et al. Improved antioxidant activity and physicochemical properties of curcumin by adding ovalbumin and its structural characterization. **Food Hydrocolloids**, v. 72, p. 304–311, 2017b.

LIU, Y. et al. Ovalbumin as a carrier to significantly enhance the aqueous solubilityand photostability of curcumin: Interaction and bindingmechanism study. **International Journal of Biological Macromolecules**, v. 116, n. May 2018, p. 893–900, 2018.

MAŁACZEWSKA, J. et al. Antiviral effects of nisin, lysozyme, lactoferrin and their mixtures against bovine viral diarrhoea virus. **BMC Veterinary Research**, v. 15, n. 1, p. 1–12, 2019.

MANDEVILLE, J. S.; FROEHLICH, E.; TAJMIR-RIAHI, H. A. Study of curcumin and genistein interactions with human serum albumin. **Journal of Pharmaceutical and Biomedical Analysis**, v. 49, n. 2, p. 468–474, 20 fev. 2009.

MATHEW, D.; HSU, W. Antiviral potential of curcumin. **Journal of Functional Foods**, v. 40, n. September 2017, p. 692–699, 2018.

MOHAMMADI, F. et al. Interaction of curcumin and diacetylcurcumin with the lipocalin member β-lactoglobulin. **Protein Journal**, v. 28, n. 3–4, p. 117–123, maio

2009.

MOHAMMADI, F. et al. Inhibition of amyloid fibrillation of hen egg-white lysozyme by the natural and synthetic curcuminoids. **RSC Advances**, v. 6, n. 28, p. 23148–23160, 2016.

MOHAMMADI, F.; MOEENI, M. Study on the interactions of trans-resveratrol and curcumin with bovine α -lactalbumin by spectroscopic analysis and molecular docking. **Materials Science and Engineering C**, v. 50, p. 358–366, 2015.

MONDAL, S.; GHOSH, S.; MOULIK, S. P. Stability of curcumin in different solvent and solution media: UV–visible and steady-state fluorescence spectral study. **Journal of Photochemistry and Photobiology B: Biology**, v. 158, p. 212–218, 2016.

NADI, M. M. et al. Comparative Spectroscopic Studies on Curcumin Stabilization by Association to Bovine Serum Albumin and Casein: A Perspective on Drug-Delivery Application. **International Journal of Food Properties**, v. 18, n. 3, p. 638–659, 4 mar. 2015.

NAKSURIYA, O. et al. Curcumin nanoformulations : A review of pharmaceutical properties and preclinical studies and clinical data related to cancer treatment. **Biomaterials**, v. 35, p. 3365–3383, 2014.

NAKSURIYA, O. et al. A kinetic degradation study of curcumin in its free form and loaded in polymeric micelles. **AAPS Journal**, v. 18, n. 3, p. 777–787, 2016.

NATTRESS, F. M.; YOST, C. K.; BAKER, L. P. Evaluation of the ability of lysozyme and nisin to control meat spoilage bacteria. **International Journal of Food Microbiology**, v. 70, n. 1–2, p. 111–119, 22 out. 2001.

NEGI, P. S. et al. Antibacterial Activity of Turmeric Oil A Byproduct from Curcumin Manufacture - Journal of Agricultural and Food Chemistry (ACS

Publications). **J. Agric. Food Chem**, v. 47, p. 4297−4300, 1999.

NGUYEN, H. H. et al. Surface Plasmon Resonance: A Versatile Technique for Biosensor Applications. **Sensors**, v. 15, p. 10481–10510, 2015.

NIGEN, M. et al. Temperature affects the supramolecular structures resulting from α-lactalbumin - Lysozyme interaction. **Biochemistry**, v. 46, n. 5, p. 1248–1255, 2007.

NUNES, N. M. et al. Interaction of cinnamic acid and methyl cinnamate with bovine serum albumin: A thermodynamic approach. **Food Chemistry**, v. 237, n. 2017, p. 525–531, 2017.

NUNES, N. M. et al. Surface plasmon resonance study of interaction between lactoferrin and naringin. **Food Chemistry**, v. 297, n. April, p. 125022, 2019.

PAIVA, P. H. C. et al. Influence of protein conformation and selected Hofmeister salts on bovine serum albumin/lutein complex formation. **Food Chemistry**, v. 305, p. 125463, 1 fev. 2020.

PAN, Y. et al. Effect of barrier properties of zein colloidal particles and oil-in-water emulsions on oxidative stability of encapsulated bioactive compounds. **Food Hydrocolloids**, v. 43, p. 82–90, 1 jan. 2015.

PARROT, J.-L.; NICOT, G. Antihistaminic Action of Lysozyme. **Nature**, v. 197, n. February 2, p. 496, 1963a.

PARROT, J.-L.; NICOT, G. Antihistaminic Action of Lysozyme. **Nature**, v. 197, n. February 1963, p. 496, 1963b.

PATRA, D.; BARAKAT, C. Molecular and Biomolecular Spectroscopy Synchronous fluorescence spectroscopic study of solvatochromic curcumin dye. **Spectrochimica Acta Part A**, v. 79, p. 1034–1041, 2011.

PRASAD, S.; TYAGI, A. K.; AGGARWAL, B. B. **Recent developments in**

delivery, bioavailability, absorption and metabolism of curcumin: The golden pigment from golden spiceCancer Research and Treatment, 2014.

PU, C. et al. Stability enhancement efficiency of surface decoration on curcumin-loaded liposomes : Comparison of guar gum and its cationic counterpart. **Food Hydrocolloids**, v. 87, n. April 2018, p. 29–37, 2019.

PULIDO-MORAN, M.; MORENO-FERNANDEZ, J.; RAMIREZ-TORTOSA, CESAR RAMIREZ-TORTOSA, M. Curcumin and Health. **Molecules**, v. 21, n. 3, p. 1–22, 2016.

PULLA REDDY, A. C. et al. Interaction of curcumin with human serum albumin—A spectroscopic study. **Lipids**, v. 34, n. 10, p. 1025–1029, out. 1999.

REZENDE, J. DE P. et al. Thermodynamic and kinetic study of epigallocatechin-3-gallate-bovine lactoferrin complex formation determined by surface plasmon resonance (SPR): A comparative study with fluorescence spectroscopy. **Food Hydrocolloids**, v. 95, p. 526–532, 1 out. 2019.

REZENDE, J. DE P. et al. Human serum albumin-resveratrol complex formation: Effect of the phenolic chemical structure on the kinetic and thermodynamic parameters of the interactions. **Food Chemistry**, v. 307, p. 125514, mar. 2020.

SAHU, A.; KASOJU, N.; BORA, U. Fluorescence Study of the Curcumin-Casein Micelle Complexation and Its Application as a Drug Nanocarrier to Cancer Cells. **Biomacromolecules**, v. 9, p. 2905–2912, 2008.

SANPHUI, P.; BOLLA, G. Curcumin , a Biological Wonder Molecule : A Crystal Engineering Point of View. **Crystal Growth & Design**, v. 18, p. 5690–5711, 2018.

SCHNEIDER, C. et al. Stability of curcumin in buffer solutions and characterization of its degradation products. **Journal of Pharmaceutical and Biomedical Analysis**, v. 15, n. 12, p. 7606–7614, 2015.

SILVA, C. E. L. et al. β-Carotene and Milk Protein Complexation: a Thermodynamic Approach and a Photo Stabilization Study. **Food and Bioprocess Technology**, v. 11, n. 3, p. 610–620, 2018.

SILVA, L. H. M. DA et al. PEO-[M(CN)5NO]x- (M) Fe, Mn, or Cr) Interaction as a Driving Force in the Partitioning of the Pentacyanonitrosylmetallate Anion in ATPS: Strong Effect of the Central Atom. v. 1, p. 11669–11678, 2008.

SNEHARANI, A. H. et al. Interaction of curcumin with ß-lactoglobulin;stability, spectroscopic analysis, and molecular modeling of the Complex. **Journal of Agricultural and Food Chemistry**, v. 58, n. 20, p. 11130–11139, 27 out. 2010.

TAKAHASHI, M. et al. Heat-denatured lysozyme could be a novel disinfectant for reducing hepatitis A virus and murine norovirus on berry fruit. **International Journal of Food Microbiology**, v. 266, n. July 2017, p. 104–108, 2018.

VIEIRA, E. D.; BASSO, L. G. M.; COSTA-FILHO, A. J. Biochimica et Biophysica Acta Non-linear van ' t Hoff behavior in pulmonary surfactant model membranes. **BBA - Biomembranes**, v. 1859, n. 6, p. 1133–1143, 2017.

WANG, S.; LIU, K.; LEE, W. Effect of curcumin on the amyloid fibrillogenesis of hen egg-white lysozyme. **Biophysical Chemistry**, v. 144, n. 1–2, p. 78–87, 2009.

WANG, Y.-Q.; CHEN, T.-T.; ZHANG, H.-M. Investigation of the interactions of lysozyme and trypsin with biphenol A using spectroscopic methods. **Spectrochimica Acta Part A: Molecular and Biomolecular Spectroscopy**, v. 75, n. 3, p. 1130–1137, mar. 2010.

WILKEN, L. R.; NIKOLOV, Z. L. Process evaluations and economic analyses of recombinant human lysozyme and hen egg-white lysozyme purifications. **Biotechnology Progress**, v. 27, n. 3, p. 733–743, maio 2011.

WU, H. et al. Purification and Characterization of Recombinant Human

Lysozyme from Eggs of Transgenic Chickens. **PLOS ONE**, 2015.

WU, T. et al. What is new in lysozyme research and its application in food industry ? A review. **Food Chemistry**, v. 274, n. August 2018, p. 698–709, 2019.

YUJIA, L. et al. Improved antioxidant activity and physicochemical properties of curcumin by adding ovalbumin and its structural characterization. **Food Hydrocolloids**, v. 72, p. 304–311, 2017.